PARAMETER ESTIMATION IN HETEROGENEOUS CATALYSIS

by

Alexander K. Bonsu

Under the Supervision of Dr. O.M. Fuller

A Thesis Submitted to the
Faculty of Graduate Studies and Research
in Partial Fulfilment of the Requirements
for the Degree of Master of Engineering

Department of Chemical Engineering
McGill University
Montreal, Quebec

October 1975

I dedicate this thesis to all those who have contributed in diverse ways to bring me up, especially, my mother, Madam Afua Nyame. Her toils, guidance and prayers have made me what I am.

ABSTRACT

A mathematical model based on the concentration of the product for the estimation of the parameters characterizing the phenomena which occur during heterogeneous catalysis, has been developed. One could estimate the slopes of sorptional isotherms for the pure reactant from the mathematical model if we know the slopes of the sorptional isotherm for the pure product and if we assume the Langmuir-Hinslelwood mechanism.

The mathematical model was tested with a CSVCR (gradient-less) system using the stimulus-response technique. The reaction was the isomerization of cyclopropane to propylene in the presence of 13x zeolite catalyst.

The estimated integral average values of the first order reaction rate $\tilde{k}$ and the intra-particle diffusivity $\tilde{D}$ were compared with those reported by Kelly (1); and a very good agreement was observed. The mathematical model used in this study to calculate these values was based on the product concentration, while that of Kelly's was based on the concentration of the reactant. The estimated activation energy, 31.1 kcal/g-mole compares favorably with the results of previous investigators (1,59).

RESUME

Un modèle mathématique, basé sur la concentration du produit pour l'estimation des paramètres caractérisant les phénomènes se produisant durant la catalyse hétérogène, a été élaboré. On peut estimer les pentes des isothermes de sorption pour le réactif pur à partir du modèle mathématique si on connait les pentes des isothermes de sorption pour le produit pur et si l'on prend l'hypothèse du mécanisme de Langmuir-Hinshelwood.

Le modèle a été essayé avec un réacteur sans gradient (CSVCR) utilisant la technique de réponse impulsionnelle. La réaction était l'isomérisation de cyclopropane en propylène en présence de 13X zéolite comme catalyseur.

Les valeurs, estimées par la méthode de la moyenne intégrale, du taux de réaction du premier ordre $\tilde{k}$ et de la diffusivité intra-particulaire $\tilde{D}$ ont été comparées avec celles relevées par Kelly (1), et une très bonne concordance a été observée. Le modèle mathématique utilisé dans cette étude pour calculer ces valeurs est basé sur la concentration du produit tandis que celui de Kelly était basé sur la concentration du réactif. L'estimation de l'énergie d'activation, 31.1 kcal/g-mole, est comparée favorablement avec les résultats de précédents travaux (1,59).

ACKNOWLEDGEMENTS

The author has the greatest pleasure to acknowledge his sincere gratitude and appreciation to the guidance and advice offered by the project supervisor, Dr. O.M. Fuller. He was really helpful.

The author would also like to express his sincere thanks to Dr. J.F. Kelly for his tremendous contribution to the success of this project. The author is especially grateful to him for allowing him to use his equipment.

The contribution of Dr. M.E. Weber and Dr. Yani Doganoglu to this project is worth mentioning. They spent part of their precious time to read and to discuss the project proposals and the progress report.

The author is also thankful to the National Research Council of Canada for financial support.

Lastly, but not the least, the author would like to thank all those who, in diverse ways, contributed to this thesis.

TABLE OF CONTENTS

LIST OF ILLUSTRATIONS

LIST OF TABLES

NOMENCLATURE

A	surface area of catalyst layer exposed to the fluid phase, cm^2
c	deviation value of the effective concentration in the catalyst phase, g-mole/cm^3 catalyst volume
C	total (sum of steady state and deviation values) effective concentration in the catalyst layer, g-mole/cm^3 catalyst volume
$\overline{C}$	steady state effective concentration in the catalyst layer, g-mole/cm^3 catalyst volume
C_T	constant in the Langmuir sorption isotherm expression (Equation 5-56 and Equation 5-57), equivalent to the total sorbate capacity of the catalyst layer at saturation, g-mole/cm^3 catalyst volume
D	effective intra-particle diffusivity, cm^2/sec
$\tilde{D}$	integral average value of D, cm^2/sec
F	total volumetric flow rate into and out of the reactor, cm^3/sec
h	length parameter in catalyst layer, ratio of the catalyst volume (V*) to outside surface area (A), cm
H(s)	reactor transfer function
k	intrinsic first-order reaction rate constant per unit volume of catalyst layer, sec^{-1}
$\tilde{k}$	integral average value of k, sec^{-1}
K_c	equilibrium Langmuir adsorption constant for reactant, cyclopropane, defined by Equation 5-56, dimensionless
K_p	equilibrium Langmuir adsorption constant for product, propylene, defined by Equation 5-57, dimensionless
M	magnitude of square wave forcing function, g-mole/cm^3
N	parameter group defined by Equation 3-41, sec
P_T	total internal reactor or CSV system pressure, mm Hg
Q	parameter group defined by Equation 3-40, sec^{-1}

RF	parameter group defined by Equation 5-47, cm^3/sec
RR	parameter group defined by Equation 3-33
RP	parameter group defined by Equation 3-42
S	Laplace transform variable
t	independent time variable, sec
V^+	volume of the fluid phase, cm^3
W	duration of square wave forcing pulse, sec
x	deviation value of the input (forcing) concentration in the fluid phase, $g\text{-moles}/cm^3$
X	total (sum of steady state and deviation values) input concentration in the fluid phase, $g\text{-mole}/cm^3$
y	deviation value of the output concentration in the fluid phase, $g\text{-mole}/cm^3$
Y	total (sum of steady state and deviation values) output concentration in the fluid phase, $g\text{-mole}/cm^3$
z	independent dimensionless distance variable in the catalyst layer

GREEK LETTERS

α	$A\psi/F$, sec/cm^{-1}
β	$\sqrt{k/D}$, cm^{-1}
γ	$\psi\sqrt{Dk}$, $cm\ sec^{-1}$
ϕ	$h\sqrt{k/D}$, Thiele modulus
τ	residence time, sec
ψ	slope of sorption isotherm about the steady state value fluid phase concentration
μ_n	n^{th} unnormalized moment about the origin of the reactor fluid phase (y(t)) response, $g\text{-mole}\ sec^{n\ 1}/cm^3$
η	constant, defined by Equation 5-64

SUPERSCRIPTS

$\bar{}$	indicates steady state values
$\hat{}$	indicates normalized moment
+	indicates fluid phase
*	indicates catalyst layer
$\sim$	indicates Laplace transformed variable

SUBSCRIPTS

1	indicates thin pellet
2	indicates thick pellet
Δ	indicates reactant, cyclopropane
p	indicates product, propylene
N	indicates inert, nitrogen

1. GENERAL INTRODUCTION

Heterogeneous catalytic reactors are widely used in the chemical industries. The design of this type of reactor requires the knowledge of the parameters which account for mass transfer, sorption, and reaction phenomena. Thus it is essential to develop a simple, but efficient method for estimating these parameters.

Kelly (1) developed a method that depended on the measurement and interpretation of reactant concentration. While the method produced reasonable reaction rate coefficients, the variability of the data was undesirably large. The purposes of this project were to test Kelly's model by an alternate method based on product concentration and to reduce the variability of the data.

The equipment used was the same as the one used by Kelly (1). There was only one major difference in the experimental procedure. Kelly (1) used a mixture of the reactant and product in the feed gas to the reactor. In this study a mixture of the reactant and inert gas was used as the feed gas to the reactor.

The effluent gas from the reactor consisted of the reactant, product and inert gas. The infra-red spectrophotometer was used to monitor its composition. Being interested in only the product concentration, a suitable wavelength (6.1 μ) was chosen at which the product was strongly absorbing while the reactant was non-absorbing. The inert gas (i.e. nitrogen) posed no problem in the search for this wavelength. The reason is that nitrogen is completely transparent throughout the infra-red spectrum.

2. LITERATURE SURVEY

The earliest investigations in the field of heterogeneous catalysis used microcatalytic (2,3,4) and gas chromatographic (5,6,7) techniques. These two techniques were combined by Bassett and Habgood (2) to study the isomerization of cyclopropane to propylene on a molecular sieve catalyst. A detailed review of these early investigations and some recent studies has been presented by Kelly (1).

The models which had been developed by most authors (9-18) did not include reaction phenomena . However, they all accounted for sorption and diffusion phenomena. In some of the models (9,10,12) axial dispersion and external mass transfer were considered.

For a realistic approach to heterogeneous catalysis in a fixed bed or gas chromatographic reactor, we must account for five phenomena, namely: particle-to-fluid mass transfer, axial dispersion, intra-particle diffusion, sorption and reaction. However,complex equations arise when all the five phenomena are considered. Hence most investigators develop methods where two or three of the phenomena are significant while the rest are neglected. A list of the authors and the various phenomena that they considered in their methods is presented in Table 2-1.

Recently, Kawazoe et.al. (19) used the chromatographic method to study the adsorption of nitrogen on molecular sieve carbon. The adsorption isotherms were non-linear. Thus a small perturbation pulse of nitrogen was introduced to the steady flow of a given nitrogen concentration. The response was analysed using the theory of non-equilibrium

TABLE 2-1

List of Investigators and the Phenomena they Considered

Author (Ref.)	Axial Dispersion	Particle-to-Fluid Mass Transfer	Intra-Particle Diffusion	Sorption	Reaction
Thomas (49)			*		
Roser (31)			*		
Dogu and Smith (25)			*		
Edeskuty and Amundson			*		
Roser (32)			*	*	
Masamuna and Smith (11)			*	*	
Smith and co-workers (14-18)			*	*	
Kawazoe, Suzuki and Chihara (19)			*	*	
Kocirik (36)			*	*	*
Roginskii and Rozental (37)			*	*	*
Donisova and Rozental (38)			*	*	*
Kubin (9)	*	*	*	*	
Kucera (10)	*	*	*	*	
Suzuki and Smith (16)	*	*	*	*	
Padberg and Smith (13)	*	*	*	*	
Kelly (1)			*	*	*

chromatography. The apparent adsorption equilibrium constants were determined from the retention times of the peaks for different steady flow concentrations. The peak width was used to estimate the intra-microparticle diffusivity. The strong dependence of the diffusivity on the amount adsorbed was explained in terms of the chemical potential gradient. The chemical potential gradient acted as a driving force of the diffusion.

A pulse reactor with a heat-flow micro-calorimeter had been developed quite recently (20,21). This technique allows both kinetic-related and thermal information to be obtained.

In addition to the micro-reactor and gas chromatography, the single pellet reactor has also emerged. Its theory and experimental procedure at steady state have been developed by Balder and Peterson (22). Gibilaro et al. (23) have also proposed the transient procedure for investigating the pore structure.

Suzuki and Smith (24) used the single pellet with a well mixed gas phase to investigate the adsorption phenomenon. With their experimental model, all other types of mass transfer were eliminated, except intra-particle mass transfer. They estimated the adsorption equilibria data from first moments. Adsorbable tracer was used. According to the authors, the measurement from pellets of different thickness could be used to estimate both the effective diffusivity and adsorption equilibrium constant.

Dogu and Smith (25) very recently developed a simple and rapid technique for the determination of effective diffusivity of catalysts

using pulse-response technique. They used the Wicke-Kallenbachtype of diffusion cell. Their results could be very reliable if the retention time in the dead volumes could be made to be negligible compared to the diffusion time in the pellet. Another problem with the Wicke-Kallenbach diffusion cell is the bypassing along the sides of the pellet which becomes significant at high temperatures.

Kelly (1) recently developed a method which allows the simultaneous estimation of the parameters of diffusion, sorption and reaction phenomena. The method was based on the dynamic model and a continuous stirred-volume reactor (CSVCR) or gradientless reactor. The use of this type of reactor for heterogeneous catalysis investigation was first suggested by Bennett (26). In the gradientless type of reactor, the bulk fluid concentration is uniform and constant at steady flow of a given inlet gas concentration. The uniformity is due to the efficient mixing of the fluid phase. This makes the interfacial mass transfer resistance negligible compared to the diffusion and reaction rate resistance.

3. THEORY

3.1 Introduction

The theory for a continuous, stirred-volume, catalytic reactor (CSVCR) has been developed by a number of authors (24,26-29). Kelly and Fuller (30) developed the lumped variable equilibrium model for a CSVC reactor. They assumed a first-order reaction. Kelly (1) later developed the lumped variable non-equilibrium model and the distributed variable model.

In the lumped variable models, the concentration of the reactant (or product) in the catalyst phase was characterized by an effective concentration. The effective concentration represented both the sorbed and non-sorbed concentrations in the pores. This definition coupled with the fact that the measurable gas phase concentration is uniform permits the functional form of the adsorption isotherm to be obtained. This then allows the experimentation to be carried out at all inlet reactant concentrations.

In the distributed variable model, the reactant is distributed between gas and sorbed phases inside the pores of the catalyst pellet. If a Taylor series expansion is used to linearize the adsorption term in this model, the adsorption coefficient will be a function of displacement from the boundary between the porous catalyst and the bulk fluid phase. The reason for this is that the pore gas phase concentration varies with position in the catalyst layer. For the limiting case where the concentration difference in the gas phase in the pores is negligible

and external mass transport resistance is also negligible, the Taylor series approach may be used. However, this would preclude the measurement of effective intra-pellet diffusivities.

The disadvantage of the distributed variable model is that each component in the catalyst layer must be described by two differential equations. The lumped variable models require only a single equation. Hence, in the present investigation, where two components (product and reactant) must be considered, the lumped variable model proved to be the most appropriate to use. The lumped-variable non-equilibrium model is a more complete description of the phenomena than the equilibrium model when considering a reaction system. However, the expressions for the moments of the non-equilibrium model are too complex for practical application. Hence, only the lumped-variable equilibrium model was used.

3.2 Lumped Variable Equilibrium Model

3.2.1 Basic equations

i. Catalyst Layer

The irreversible first-order reaction to be considered is given by

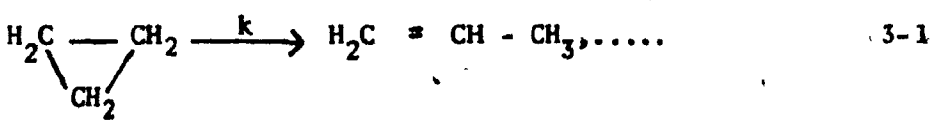

$$H_2C \underset{CH_2}{\overset{CH_2}{—}} \xrightarrow{k} H_2C = CH - CH_3, \quad \text{..... 3-1}$$

cyclopropane — propylene

where k is the reaction rate constant. The reaction is athermal (1) and since moles are conserved, there should be no temperature and pressure gradients.

The continuity equations for the reactant product and inert gas in the catalyst phase in terms of the deviation variables are given by

$$\frac{\partial c_{\Delta}}{\partial t}(z,t) = \frac{D}{h^2}\frac{\partial^2 c_{\Delta}}{\partial z^2}(z,t) - kc_{\Delta}(z,t) \qquad 3\text{-}2$$

$$\frac{\partial c_{P}}{\partial t}(z,t) = \frac{D}{h^2}\frac{\partial^2 c_{P}}{\partial z^2}(z,t) + kc_{\Delta}(z,t) \qquad 3\text{-}3$$

$$\frac{\partial c_{N}}{\partial t}(z,t) = \frac{D}{h^2}\frac{\partial^2 c_{P}}{\partial z^2}(z,t) \qquad 3\text{-}4$$

The deviation variables are the small change in concentration about the steady state values:

$$\text{i.e.} \quad c(t) = C(t) - \bar{C} \qquad 3\text{-}4A$$

where c is deviation value,

C is total value,

$\bar{C}$ is steady state value, and

t is time.

The effective intra-particle diffusivity, D, is defined as the ratio of the diffusion flux density to the effective concentration gradient, where the flux density is based on the total cross-sectional area of the catalyst layer. The diffusivity is assumed to be independent of concentration. It is also assumed to be the same for the reactant, product and inert gas. For uniform catalyst texture achieved by wet pressing of the pellet, D is independent of z, the independent dimensionless distance variable in the catalyst layer and t, time.

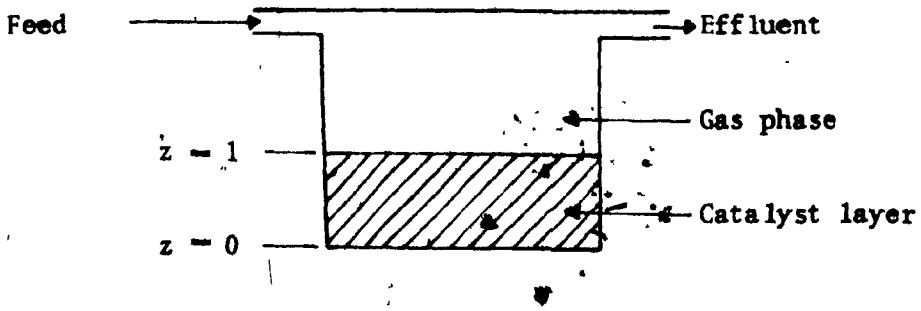

SCHEMATIC DIAGRAM OF CSVCR

The dependent variable we want to solve for is the concentration of the product, c_p, contained in Equation 3-3. However, this equation cannot be solved alone. It contains one more dependent variable, namely c_Δ, which is the concentration of the reactant in the reaction term. However the reaction term is eliminated when Equations 3-2 and 3-3 are added. And by defining a new variable,

$$c = c_\Delta + c_p \qquad 3\text{-}5$$

we obtain

$$\frac{\partial c}{\partial t}(z,t) = \frac{D}{h^2}\frac{\partial^2 c}{\partial z^2}(z,t) \qquad 3\text{-}6$$

The boundary conditions for Equations 3-2 and 3-3 and hence Equation 3-6 are given by:

B.C. 1 $$c_\Delta(1,t) = \psi_\Delta y_\Delta(t) \qquad 3\text{-}7a$$

$$c_p(1,t) = \psi_p y_p(t) \qquad 3\text{-}7b$$

$$c(1,t) = \psi_\Delta y_\Delta(t) + \psi_p y_p(t) \qquad 3\text{-}7c$$

These boundary conditions assume that there is linear relationship between a small change in the gas phase concentration, y(t), about the

steady state value $\bar{Y}$ and the corresponding change in the amount adsorbed on the pellet surface, c(1,t). ψ_Δ and ψ_p are the slopes of the sorption isotherms for the reactant and product respectively. A more elaborate version of these boundary conditions will be discussed in Section 5.2.

B.C. 2 $$\frac{\partial c_\Delta}{\partial t}(0,t) = 0 \qquad 3\text{-}8a$$

$$\frac{\partial c_p}{\partial t}(0,t) = 0 \qquad 3\text{-}8b$$

$$\frac{\partial c}{\partial t}(0,t) = 0 \qquad 3\text{-}8c$$

The second group of boundary conditions represents the fact that there is no mass transfer through the sealed end of the catalyst layer.

The initial conditions are given by

I.C. $$c_\Delta(z,0) = 0 \qquad 3\text{-}9a$$

$$c_p(z,0) = 0 \qquad 3\text{-}9b$$

$$c(z,0) = 0 \qquad 3\text{-}9c$$

These conditions indicate that at time, t = 0, the system is at steady state and there is no transient change in concentration.

ii. Gas Phase

Conservation of mass equations describing the reactant, the reactant product and their sum in the gas phase are given by:

$$V\frac{dy_\Delta}{dt} = F(x_\Delta - y_\Delta) - \frac{AD}{h}\left(\frac{\partial c_\Delta}{\partial z}\right)_{z=1} \qquad 3\text{-}10a$$

$$V^+\frac{dy_p}{dt} = F(x_p - y_p) - \frac{AD}{h}\left(\frac{\partial c_p}{\partial z}\right)_{z=1} \qquad 3\text{-}10b$$

$$V^+\frac{dy}{dt} = F(x-y) - \frac{AD}{h}\left(\frac{\partial c}{\partial z}\right)_{z=1} \qquad 3\text{-}10c$$

where $x = x_\Delta + x_p$ 3-11a

$y = y_\Delta + y_p$ 3-11b

and V^+ is the volume of the gas phase.

The initial conditions are given by:

$y_\Delta(0) = 0$ 3-12a

$y_p(0) = 0$ 3-12b

$y(0) = 0$ 3-12c

3.2.2 Solution in Laplace domain

i. Catalyst Layer

Transforming Equations 3-6, 3-7c, 3-8c and 3-9c to the Laplace domain and solving for C(s) gives

$$\tilde{C}(s) = \frac{\psi_\Delta \tilde{Y}_\Delta(s) + \psi_p \tilde{Y}_p(s)}{\text{Cosh}(h\sqrt{s/D})}\,\text{Cosh}(hz\sqrt{s/D}) \qquad 3\text{-}13$$

The solution for $\tilde{c}_\Delta(s)$ in the Laplace domain is given by

$$\tilde{c}_\Delta(s) = \psi_\Delta \tilde{Y}_\Delta(s)\frac{\text{Cosh}(hz\sqrt{(k+s)/D})}{\text{Cosh}(h\sqrt{(k+s)/D})} \qquad 3\text{-}14$$

Hence

$$\tilde{c}_p(s) = \frac{\psi_\Delta \tilde{Y}_\Delta(s) + \psi_p \tilde{Y}_p(s)}{\text{Cosh}(h\sqrt{s/D})}\text{Cosh}(hz\sqrt{s/D}) - \psi_\Delta \tilde{Y}_\Delta(s)\frac{\text{Cosh}(hz\sqrt{(k+s)/D})}{\text{Cosh}(h\sqrt{(k+s)/D})}$$

.....3-15

ii. Gas Phase

The Laplace transform of Equation 3-10b is given by

$$V^{+}\tilde{Y}_p(s) = F(\tilde{X}_p(s)-\tilde{Y}_p(s)) - \frac{AD}{h}\left(\frac{\partial \tilde{C}_p}{\partial z}\right)_{z=1} \qquad 3\text{-}16$$

From Equation 3-15 we have

$$\left(\frac{\partial \tilde{C}_p}{\partial z}\right)_{z=1} = \left[\psi_\Delta \tilde{Y}_\Delta(s)+\psi_p \tilde{Y}_p(s)\right](h\sqrt{s/D})\tanh(h\sqrt{s/D}) - \psi_\Delta \tilde{Y}_\Delta(s) h\sqrt{(k+s)/D}\,\tanh(h\sqrt{(k+s)/D}) \quad \ldots\ldots 3\text{-}17$$

Substituting Equation 3-17 in Equation 3-16 and then dividing through by F gives

$$\tau^{+}s\tilde{Y}_p(s) = \tilde{X}_p(s)-\tilde{Y}_p(s)- \frac{AD}{F}\{\left[\psi_\Delta \tilde{Y}_\Delta(s) + \psi_p \tilde{Y}_p(s)\right]\sqrt{s/D}\,\tanh(h\sqrt{s/D}) - \psi_\Delta \tilde{Y}_\Delta(s)\sqrt{(k+s)/D}\,\tanh(h\sqrt{(k+s)/D})\} \qquad 3\text{-}18$$

where $\tau^{+} = V^{+}/F$.

By solving the Laplace transform of Equations 3-2, 3-10a and their appropriate boundary and initial conditions we obtain

$$\tilde{Y}_\Delta(s) = \frac{\tilde{X}_\Delta(s)}{1 + \tau^{+}s + \frac{A}{F}\psi_\Delta\sqrt{D(k+s)}\,\tanh(h\sqrt{k+s)/D})} \qquad 3\text{-}19$$

The following transfer function is obtained after substituting Equation 3-19 in Equation 3-18, and assuming no product in the input gas (i.e. $\tilde{X}_p(s) = 0$):

$$H_{p\Delta}(s) = \frac{\tilde{Y}_p(s)}{\tilde{X}_\Delta(s)}$$

$$= A\frac{\psi_\Delta}{F}\left[\sqrt{D(k+s)}\tanh\left(h\sqrt{(k+s)/D}\right) - \sqrt{sD}\tanh\left(h\sqrt{s/D}\right)\right]/\{\left[1\right.$$

$$+ \tau^+ s + A\frac{\psi_\Delta}{F}\sqrt{D(k+s)}\tanh\left(h\sqrt{(k+s)/D}\right)\left[1 + \tau^+ s\right.$$

$$\left. + A\frac{\psi_p}{F}\sqrt{sD}\tanh\left(h\sqrt{s/D}\right)\right]\} \qquad \text{.....3-20}$$

3.2.3 Moments of response curves to square wave input

The experiments will consist of measuring the responses in the product concentration to square-wave stimuli in the reactant concentration as described in Section 4.2.2B. Consequently, we need to express the moments of the response curves in terms of the unknown parameters. The relationship between the moments of the response curves and the Laplace transform of the product concentration of the reactor output $Y_p(s)$ is given by

$$\mu_n = (-1)^n \lim_{s\to o} \frac{d^n \tilde{Y}_p(s)}{ds^n} \qquad 3\text{-}21$$

where $$\mu_n = \int_o^\infty y(t)t^n dt \qquad 3\text{-}22$$

For a square-wave input of the reactant concentration,

$$\tilde{X}_\Delta(s) = M(1-e^{-Ws})/s \qquad 3\text{-}23$$

where M is the magnitude of square-wave, forcing function and W is the duration.

The zeroth moment is given by

$$\mu_o = \lim_{s\to o} \tilde{Y}_p(s) = \frac{MW\alpha_\Delta\sqrt{Dk}\tanh\phi}{1\ \alpha_\Delta\sqrt{Dk}\tanh\phi} \qquad 3\text{-}24$$

where ϕ, the Thiele modulus $= h\sqrt{k/D}$ and $\alpha_\Delta = \frac{A\psi_\Delta}{F}$.

From Equation 3-24, we have

$$\alpha_\Delta \sqrt{Dk} \tanh\phi = \mu_o/(MW-\mu_o) \qquad 3\text{-}25$$

and

$$1 + \alpha_\Delta \sqrt{Dk} \tanh\phi = MW/(MW-\mu_o) \qquad 3\text{-}26$$

The first unnormalized moment μ_1 is given by

$$\mu_1 = -\lim_{s\to o} \frac{d\bar{Y}_p}{dS}(s) \qquad 3\text{-}27$$

$$= MW\alpha_\Delta \{\sqrt{Dk} \tanh\phi \left[\tau^+ + \frac{\alpha_\Delta}{2}(\sqrt{D/k} \tanh\phi + h\,\mathrm{Sech}^2\phi)\right.$$

$$\left. + (\tau^+ + \alpha_p h)(1 \alpha_\Delta \sqrt{Dk} \tanh\phi)\right]$$

$$- (1+\alpha_\Delta \sqrt{Dk} \tanh\phi)\left[1/2(\sqrt{D/k} \tanh\phi + h\,\mathrm{Sech}^2\phi - 2h)\right.$$

$$\left. - \frac{W}{2}\sqrt{Dk} \tanh\phi\right]\}/(1+\alpha_\Delta \sqrt{Dk} \tanh\phi)^2 \qquad .....3\text{-}28$$

The first normalized moment, $\hat{\mu}_1$, is

$$\hat{\mu}_1 = \mu_1/\mu_o$$

so,

$$\hat{\mu}_1 = \{\tau^+ + \frac{\alpha_\Delta}{2}(\sqrt{D/k} \tanh\phi + h\,\mathrm{Sech}^2\phi) + (1+\alpha_\Delta \tanh\phi) \times$$

$$(\tau^+ + \alpha_p h) - \frac{1+\alpha_\Delta \sqrt{Dk} \tanh\phi}{2\sqrt{Dk} \tanh\phi} \times$$

$$\left[\sqrt{D/k} \tanh\phi + h\,\mathrm{Sech}^2\phi - 2h - W\sqrt{Dk} \tanh\phi\right]\}/(1+\alpha_\Delta \sqrt{Dk} \tanh\phi)$$

$$.....3\text{-}29$$

Then, from Equations 3-25 and 3-26,

$$\hat{\mu}_1 = \tau^+(2-\mu_o/MW) + \frac{1}{2k}(\mu_o/MW-1) + \alpha_p h + W/2$$

$$+ \frac{h\alpha_\Delta}{2}(MW/\mu_o - \mu_o/MW) + (\mu_o/MW)(h/\alpha_\Delta Dk) \qquad .....3\text{-}30$$

3.2.4 Solution of the moment equations to determine the parameters

There are four parameters to be estimated; namely: 1) k, the first-order reaction rate constant, 2) D, the intragranular diffusivity, 3) ψ_Δ, the adsorption equilibrium constant for the reactant, and 4) ψ_p, the adsorption equilibrium constant for the product. ψ_Δ and ψ_p are contained in the terms α_Δ and α_p, respectively.

There are only two equations involving the zeroth and the first normalized moments (i.e. Equations 3-24 and 3-30). Hence to solve for the four parameters, the measurements from two pellet thicknesses are required.

From Equation 3-25 and for two pellets of different thicknesses h_1 and h_2, we have

$$\frac{A\gamma}{F_1}\tanh(h_1\beta) = RR_1(1-RR_1) \qquad 3\text{-}31$$

$$\frac{A\gamma}{F_2}\tanh(h_2\beta) = RR_2(1-RR_2) \qquad 3\text{-}32$$

$$RR = \mu_o/MW \qquad 3\text{-}33$$

$$\beta = \sqrt{k/D} \qquad 3\text{-}34$$

$$\gamma = \psi_\Delta\sqrt{Dk} \qquad 3\text{-}35$$

Taking the ratio of Equations 3-31 and 3-32, we have

$$\frac{\tanh(h_1\beta)}{\tanh(h_2\beta)} = \frac{RR_1F_1(1-RR_1)}{RR_2F_2(1-RR_2)} \qquad 3\text{-}36$$

Each term in Equation 3-36 can be measured independently, except β. β can be obtained by solving the above non-linear equation. Then, by substituting β in either Equation 3-31 or 3-32, we can solve for γ.

From Equations 3-34 and 3-35,

$$\psi_\Delta = \frac{\beta\gamma}{k} \qquad 3\text{-}37$$

and

$$\psi_\Delta D = \frac{\gamma}{\beta} \qquad 3\text{-}38$$

Substituting Equations 3-33, 3-37 and 3-38 in Equation 3-30 and dividing through by $\tau^*(= Ah/F)$ and rearranging we arrive at,

$$\psi_p + \frac{1}{2k}\left[(RR-1)/\tau^* + \beta\gamma(1/RR-RR) - W/2\right]$$

$$= 1/\tau^*\left[\hat{\mu}_1 - \tau^*(2-RR) - W/2\right] \qquad \text{.....}3\text{-}39$$

By defining

$$Q = 1/2\left[(RR-1)/\tau^* + \beta\gamma(1/RR-RR)\right] \qquad 3\text{-}40$$

$$N = \left(\frac{F^2\gamma}{2A^2\beta}\right)RR \qquad 3\text{-}41$$

and

$$RP = 1/\tau^*\left[\hat{\mu}_1 - \tau^*(2-RR) - W/2\right] \qquad 3\text{-}42$$

we obtain

$$\psi_p + \frac{Q}{k} + Nk = RP \qquad 3\text{-}43$$

Then, for two pellets of different thicknesses, we have

$$\psi_p + \frac{Q_1}{k} + N_1 k = RP_1 \qquad 3\text{-}44$$

$$\psi_p + \frac{Q_2}{k} + N_2 k = RP_2 \qquad 3\text{-}45$$

Subtracting Equation 3-45 from 3-44 and multiplying through by k, we obtain

$$(N_1-N_2)k^2 - (RP_1-RP_2)k + (Q_1-Q_2) = 0 \qquad 3\text{-}46$$

Equation 3-46 is a quadratic equation in terms of k which can easily be solved. We can then calculate ψ_p, ψ_Δ and D from Equations 3-44 (or 3-45), 3-37 and 3-38.

In solving either Equations 3-36 or 3-46, the data for the two pellets at the same steady state concentrations of the reactor output must be used.

4. APPARATUS AND EXPERIMENT

4.1 Apparatus

4.1.1 Introduction

The apparatus is schematically shown in Figure 4.1. It is the same apparatus used by Kelly (1). The feed streams A and B to the reactor were connected to two gas cylinders through a system of valves and connecting tubes. One of the gas cylinders contained nitrogen while the second contained cyclopropane when the reaction was being carried out. During calibration of the infra-red spectrophotometer, either the cyclopropane cylinder or the nitrogen cylinder could be replaced with propylene cylinder.

The flow rates of gases from the cylinders were set and measured by the pneumatic flow controllers and the soap bubble meters respectively. Using the manual five-way valve, the mixture of gases from the two cylinders could be fed to the reactor or by-passed to the infra-red spectrophotometer unit for the purpose of calibration. The output from the reactor could also go to the infra-red spectrophotometer for analysis.

The two major units of the apparatus are 1) the reactor, and 2) the concentration signal generator.

4.1.2 Reactor

A pictorial view of the reactor is given in Figure 4-2. The main parts are:

FIGURE 4-1 Overall schematic diagram of the feed system


: pressure measurement


: pneumatic flow controller


: manual three-way valve


: flow rate measurement by bubble meter


: manual five-way valve


: manual needle valve


: two position switching valve


: switchable union coupling

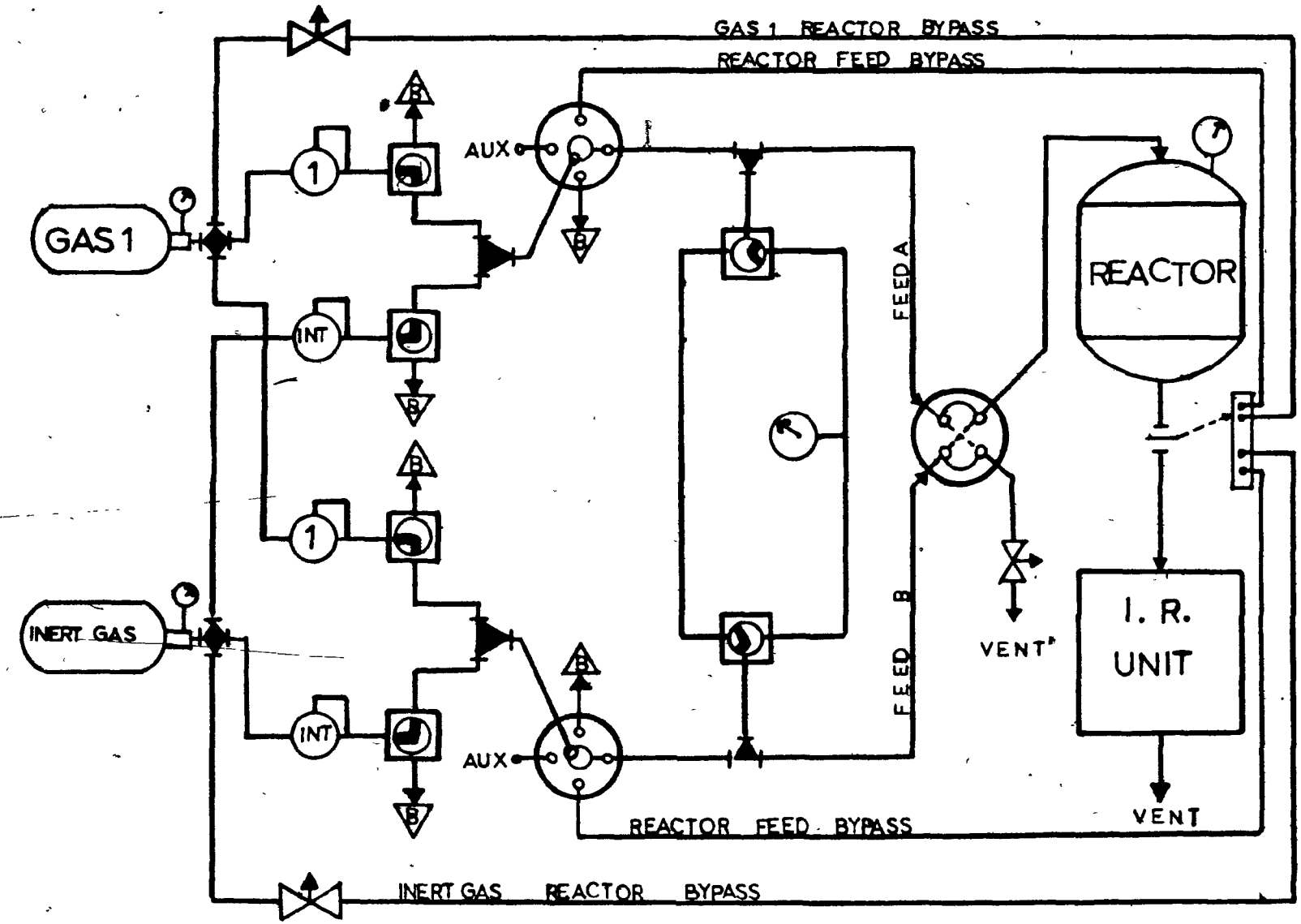
GAS 1 REACTOR BYPASS
REACTOR FEED BYPASS
AUX
GAS 1
INT
1
INERT GAS
FEED A
FEED B
REACTOR
I. R.
UNIT
VENT
VENT
AUX
REACTOR FEED BYPASS
INERT GAS REACTOR BYPASS

FIGURE 4-2 Exploded pictorial view of the CSVCR assembly

1. tacho generator
2. variable speed D.C. motor
3. motor-drive shaft coupling
4. air cylinder solenoid valves
5. drive shaft pillow block bearing
6. double acting air cylinder
7. motor-drive shaft support bracket
8. microvolume switching valve
9. thermostat insulation sections
10. external magnetic impeller
11. thermostat cartridge heater
12. outlet port
13. light pipe feedthrough
14. inlet port
15. pressure port
16. aluminum thermostat blocks
17. reactor top section
18. movable thermocouple entry
19. internal magnetic impeller
20. removable alignment pins
21. large diameter catalyst pellets
22. reactor bottom section
23. electrical disconnect

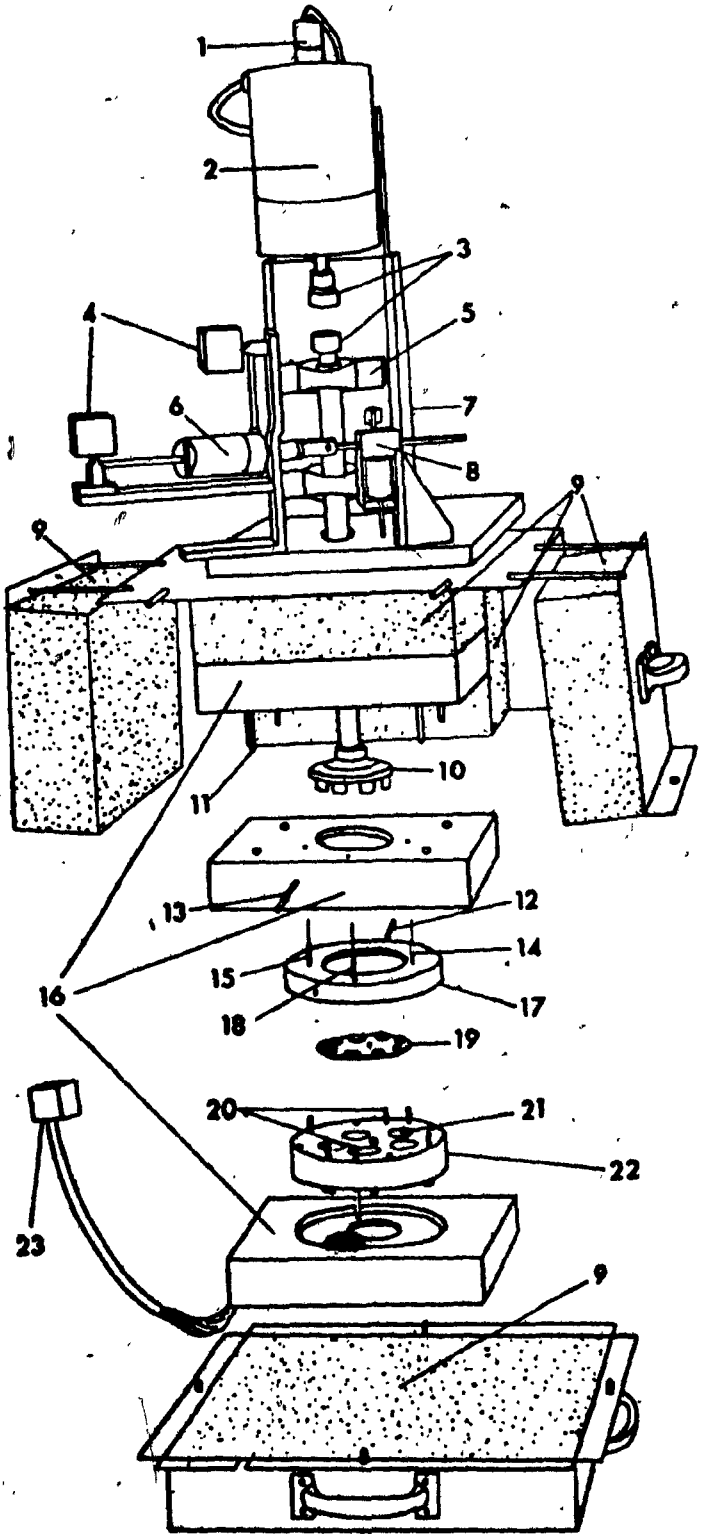
1
2
3
4
5
6
7
8
9
9
9
10
11
12
13
14
15
16
17
18
19
20
21
22
23

a) the reactor vessel, 17 and 22

b) the magnetic stirrer, 19 and 10; and

c) the thermostat, 16.

a) The reactor vessel was a disk-like cylindrical vessel of outer and inner diameters 21.91 and 15.88 cm respectively. The height was 6.35 cm. It was constructed in two parts from type 316 stainless steel. The top part, 17, was rigidly held to an aluminum thermostat block. The top part contained the magnetic stirrer, 19, the outlet and inlets, 12 and 14, pressure port, 15, and the thermocouple entries, for example, 18.

The bottom part of the reactor vessel, 22, was removable. It contained the five die holes, 21, into which the catalyst were pressed. Each die hole was 5.08 cm in diameter and 3.81 cm deep.

b) The magnetic stirrer consisted of a thin disk-like internal follower impeller, 19. It was magnetically coupled through the top part of the reactor vessel to a larger external drive impeller, 10. The internal impeller had eight Samarium Cobalt permanent magnets mounted on it. The same number of permanent magnets fitted to the external impeller were Alnico magnetic material.

At the two ends of the internal impeller shaft were two hardened, stainless-steel balls which rotated in conical bearings made from graphite-impregnated polyimide resin. The bearing cones were recessed into the two parts of the reactor vessel. The bottom cone was attached to the top of a metal bellows in a guide hole so that the cone was free to move vertically, but not to rotate. The bellows was inflated with

air pressure to force the bearing cone against the lower ball of the impeller shaft. The external impeller was driven by 0.5 horsepower, variable-speed, D.C. motor. Its axial alignment was achieved through two pillow block bearings and a large diameter shaft.

An illuminated lens was installed in the top section of the reactor vessel. A co-linear light pipe on the opposite side of the vessel permitted an observer to see the rotation of the internal impeller.

c) The thermostat consisted of three aluminum blocks, 16. They completely enveloped the reactor vessel and the external drive impeller. The heating of the aluminum blocks was done by a series of stainless steel cartridge heaters, 11. They were symmetrically distributed between the three sections of the thermostat. The temperature of the thermostat was controlled by a proportional controller plus a thermocouple sensor. The controller operated a group of trimmer heaters (320 watts). Two variable transformers were manually used to control the rest of the heaters (1500 watts). The thermostat was insulated with a high temperature fiberglass insulation panels, 9.

4.1.3 Concentration signal generator

The concentration signal generator is shown schematically in Figure 4-3. The parts are also pictorially indicated in Figure 4-2. They are air cylinder valves, 4, double acting cylinder, 6, and micro-volume, two-position, switching valve, 8.

By the activation of the switch on the electronic timer, indicated in Figure 4-3, an electrical pulse was generated. The pulse

FIGURE 4-3 Schematic diagram of the concentration signal generator

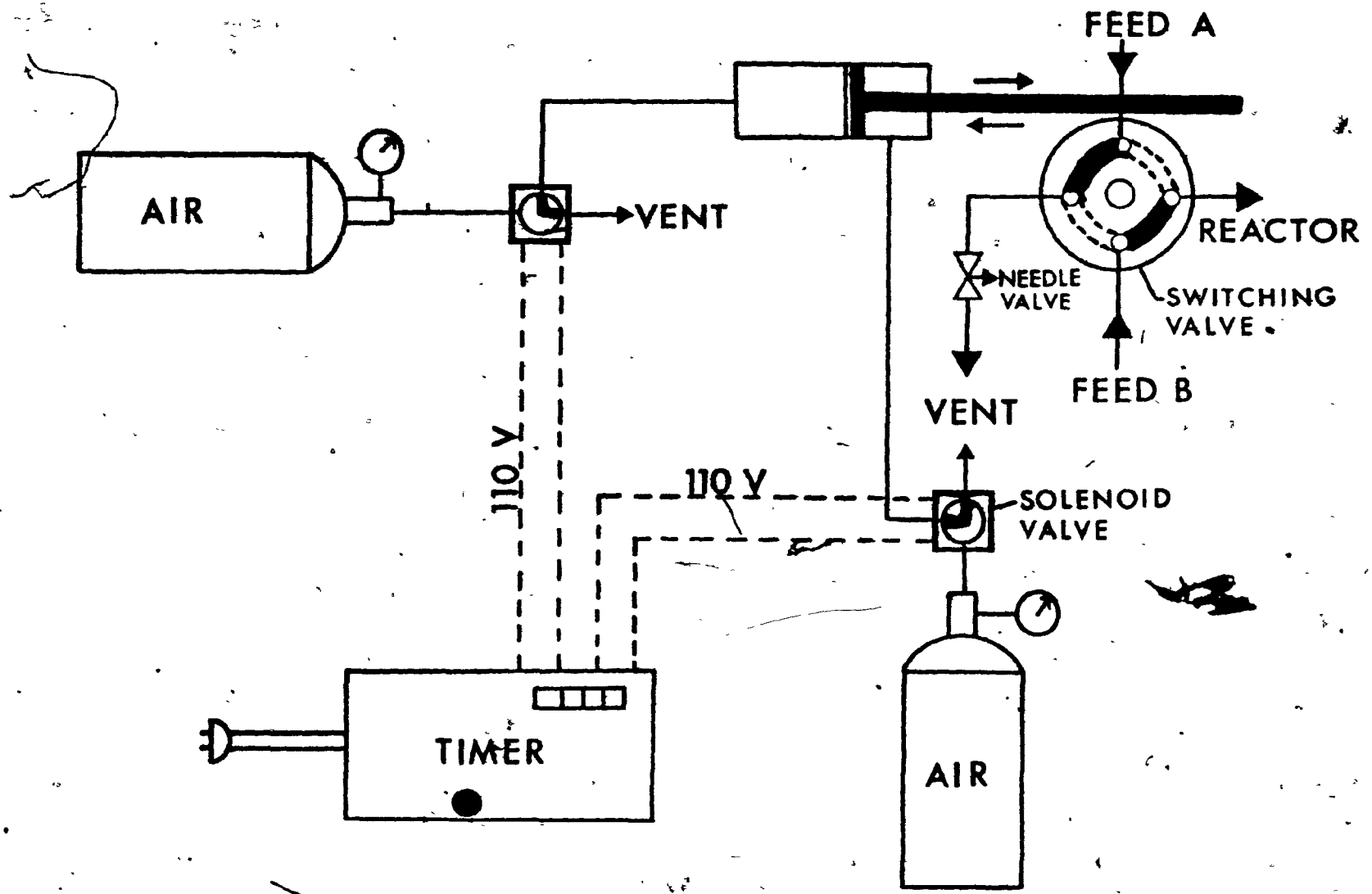
FEED A
AIR
VENT
REACTOR
NEEDLE VALVE
SWITCHING VALVE
FEED B
VENT
110 V
110 V
SOLENOID VALVE
TIMER
AIR

energized and held the start relay. This supplied power to the solenoid coils, which then rotated the solenoid-actuated three-way valve to supply air pressure to the double-acting cylinder. The shaft of the piston of the cylinder was connected to the stem of the micro-volume switching valve. Then, by means of a single stroke, the valve was rotated through an angle of 90 degrees. This rotation changed the feed stream going to the reactor.

A square wave was generated for, say, W seconds. Then at the end of this period, a second internal timer pulse energized the return relay. This then operated the second solenoid valve to return the micro-volume switching valve to its original position. Thus the original feed stream to the reactor was returned.

A cross-over switch in the output circuit of the timer allowed either solenoid valve to receive the starting pulse. The duration of the electrical pulse was 100 msec. The switching time of the micro-volume switching valve was 35 msec.

4.2 Experimental Section

4.2.1 Material

A. Catalyst Pellet

The catalyst pellet was prepared from zeolite-molecular sieve Type 13X. The ground powder of the zeolite was compressed into the five die holes of the bottom half of the reactor vessel. Sodium chloride was first pressed into the die holes before the catalyst. The purpose of this was to keep the pellet surface near to the top of the die holes.

The compression pressure was about 25,000 psi.

The zeolite powder was added to the top of the sodium chloride. It was then wetted with acetone to provide even pressure distribution within the grains during pressing. The compression pressure applied was about 23,000 psi. Both the thin and thick pellets were formed by the same procedure. To avoid the cracking of the thin pellets when they were raised to the pretreatment temperature of 300°C, they were gradually baked by heating to 60, 80, 100, 120 and 160 °C for one hour each in a vacuum oven..

The catalyst was always regenerated after each set of runs at a given reaction temperature. The regeneration was carried out in a furnace at 300°C for 12 hours. The catalyst was then cooled in a vacuum oven to 60°C.

The pellet density estimated from the dimensions and the weight of the pellet was 1.155 g/cm^3. The solid density measured with a helium pycnometer was 2.31 g/cm^3. From the two densities the average pellet porosity was estimated to be 0.500.

The details of the press assembly and the procedure are described by Kelly (1).

B. Gases

The purity of the propylene and cyclopropane supplied by Canada Liquid Air was specified to be 99.0 per cent. The nitrogen supplied by Liquid Carbonic Canada Ltd. had a guaranteed minimum purity of 99.9 per cent.

4.2.2 Procedure

A. Calibration of the Infra-red Spectrophotometer

The effluent from the reactor consisted of nitrogen, propylene and cyclopropane. But we were interested in only the concentration of the product. Hence a suitable wavelength of the infra-red spectrum was chosen at which propylene was strongly absorbing while cyclopropane was non-absorbing. Nitrogen presented no problem in the search for this wavelength, because nitrogen is completely transparent throughout the infra-red spectrum. The wavelength of 6.1 μ was found to satisfy the required condition. However this wavelength is within the water vapour absorption band (5.0 - 8.0 μ). Thus, interference from the atmospheric water vapour was possible.

With the filter set at 6.1 μ, propylene-nitrogen mixtures of known concentration were passed through the sample cell. The cell had a path length of 3 cm and a volume of 0.30 cm^3. The corresponding transmission from the infra-red unit in the form of a voltage signal was measured with a digital voltmeter. A calibration curve was established between the absorbance and the mole fraction of the absorbing gas (propylene). According to the Beer-Lambert Law this curve is expected to be a straight line. However, a slight curvature was observed. A sample of the calibration curve is presented in Figure 4-4. Because of the slight curvature, a second degree polynomial was fitted to the raw data using the method of least squares.

The calibration was carried out at the beginning of each set of runs at a given reaction temperature. This was done because there

FIGURE 4-4 Sample I.R. spectrophotometer calibration curve for the propylene- (nitrogen and cyclopropane)

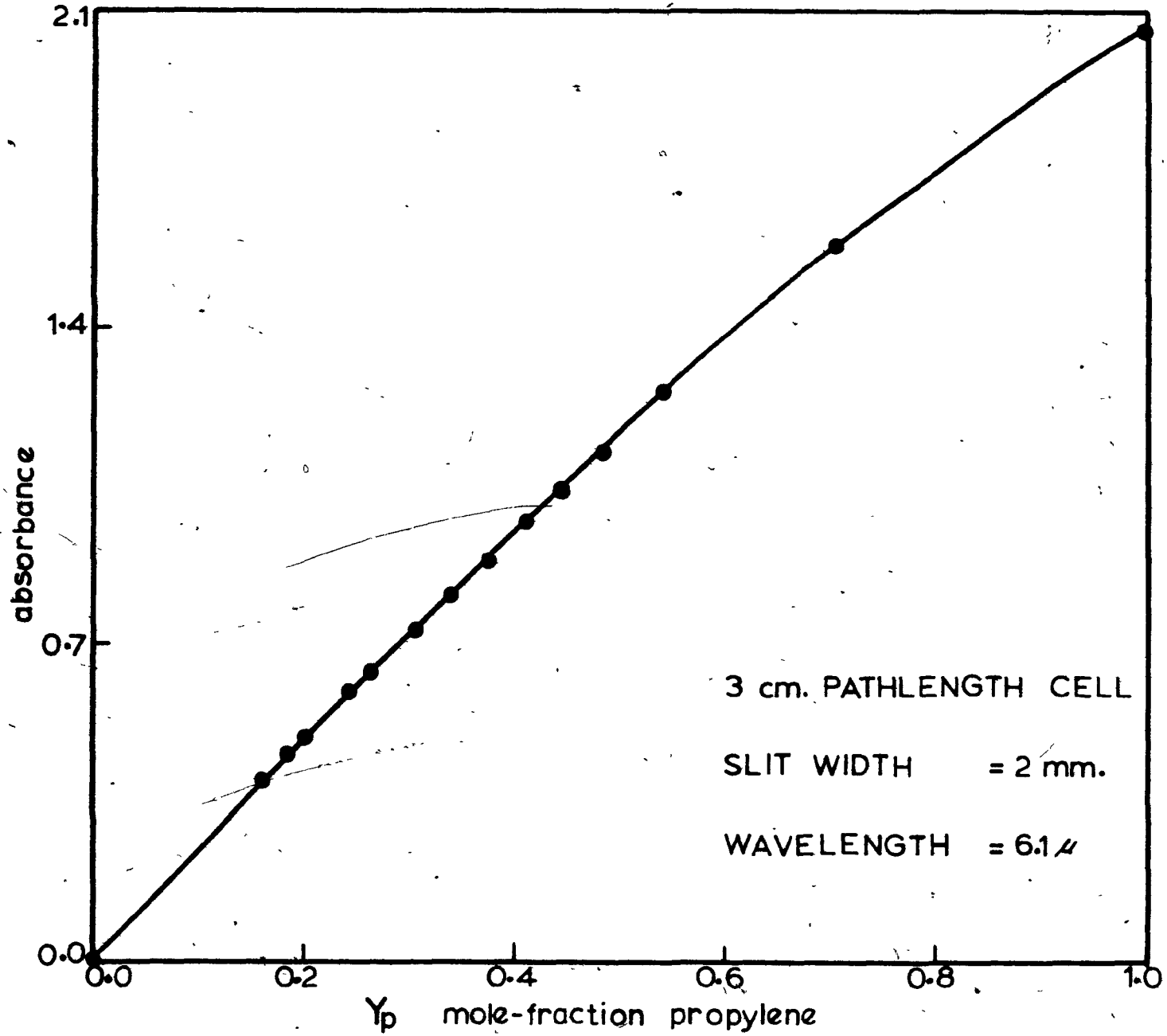
2.1
1.4
0.7
0.0
absorbance
0.0
0.2
0.4
0.6
0.8
1.0
Yp mole-fraction propylene
3 cm. PATHLENGTH CELL
SLIT WIDTH = 2 mm.
WAVELENGTH = 6.1 μ

was a slight variation in the performance of the infra-red unit. The voltage signal for the pure component changed slightly each time the experiment was run.

B. Reaction

After the pretreatment and regeneration of the catalyst pellets contained in the bottom half of the reactor vessel, the reactor was re-assembled. The reactor was then heated to the required reaction temperature. For both the thin and thick pellets, the reaction was carried out at the following three temperatures: 233°C, 243°C and 254°C.

A mixture of nitrogen and cyclopropane was passed through the reactor after it had attained a steady temperature. The flow rate of the mixture was 5.0 cm^3/sec at the ambient temperature and pressure. The composition of the mixture was estimated from the flow rate of each component in the mixture. The flow rates were measured with soap bubble meters.

The concentration of the effluent gas attained a steady state two hours after the first feed stream had been passed through the reactor. Subsequent feed streams to the reactor took around 30 minutes to reach steady state. The longer time required for the first feed stream was due to the initial fall of the activity of the catalyst to a steady state.

At steady state, a concentration square wave signal was generated by means of the set of equipment described under Section 4.1.3. Essentially it consisted of instantaneously introducing a second feed of nitrogen-cyclopropane mixture to the reactor at a different concentration. The total flow rate of the second feed stream was also maintained

at 5.0 cm^3/sec.

The concentration of the product (i.e. propylene) in the reactor output was measured continuously by passing it through the infra-red spectrophotometer. The output from the I.R. unit was in the form of a voltage signal. It was recorded on an oscillographic recorder* as a function of time.

At the end of the transient perturbation, another feed stream was introduced into the reactor to establish a new steady state. The whole procedure was then repeated again.

The mole fraction of cyclopropane in the feed was varied from 0.8 to 0.5 changing in steps of 0.1 for the thick pellet and from 0.8 to 0.4 in steps of 0.2 for the thin pellet. These steps were maintained in order to obtain a measurable difference between the steady state and transient concentrations of propylene.

The beginning of the generation of the signal was indicated by a voltage signal from the timer (Section 4.1.3) to the recorder.

The flow rate of the effluent gas was assumed to be constant and equal to the inlet flow rate in the mathematical model. To check this assumption, the effluent flow rate was measured a number of times during the transient perturbation with the soap bubble meter. The effluent flow rate was observed to vary by less than 2.0 per cent. This is within the 3.0 per cent error caused by the use of the bubble

---

*Sanborn 7702 A Recorder, Hewlett Packard.

meter for the measurement of flow rates.

In order to analyse the experimental data, measurements were also taken of the ambient temperature, the catalyst pellet temperature and the atmospheric pressure.

The calibration curve for the I.R. unit was used to estimate the concentrations of the effluent gas as function of time. The deviation concentrations were then calculated and analysed according to the algorithms derived in the mathematical model.

5. RESULTS AND INTERPRETATION

5.1 Introduction

According to the algorithms developed in the theory, five parameter groups can be calculated from the experimental data. These parameter groups are as follows:

From Equation 3-33,

$$RR_i = \mu_{o,i}/M_i W_i \qquad 5\text{-}47A$$

Equation 3-36 gives,

$$RF_i = RR_i F_i/(1-RR_i) \qquad 5\text{-}47$$

From Equation 3-39, we obtain,

$$Q_i = 0.5\ (RR_i-1)/F_i + \beta\gamma(1/RR_i-RR_i) \qquad 5\text{-}48$$

$$N_i = \frac{\gamma}{2A^2\beta} F_i^2 RR_i \qquad 5\text{-}49$$

and

$$RP_i = 1/\tau_i^*\left[\hat{\mu}_{1,i}-\tau_i(2-RR_i) - W_i/2\right] \qquad 5\text{-}50$$

where i characterizes the thin (i = 1) and thick (i = 2) pellets.

At a given reaction temperature and pellet thickness, all the runs were carried out at a constant flow rate. Therefore, all other terms in the parameter groups, RF_i, Q_i and RP_i, are constant with the exception of RR_i. Thus, one can obtain the relationship between these parameter groups and the concentration of propylene at steady state, $\bar{Y}_p$, by plotting only RR_i against $\bar{Y}_p$. These plots are

FIGURE 5-1 RR_1 and RP_1 ($T = 233.5^{\circ}C$, $h_1 = 0.132$ cm) as a function of propylene gas phase molefraction, $\bar{Y}_p$

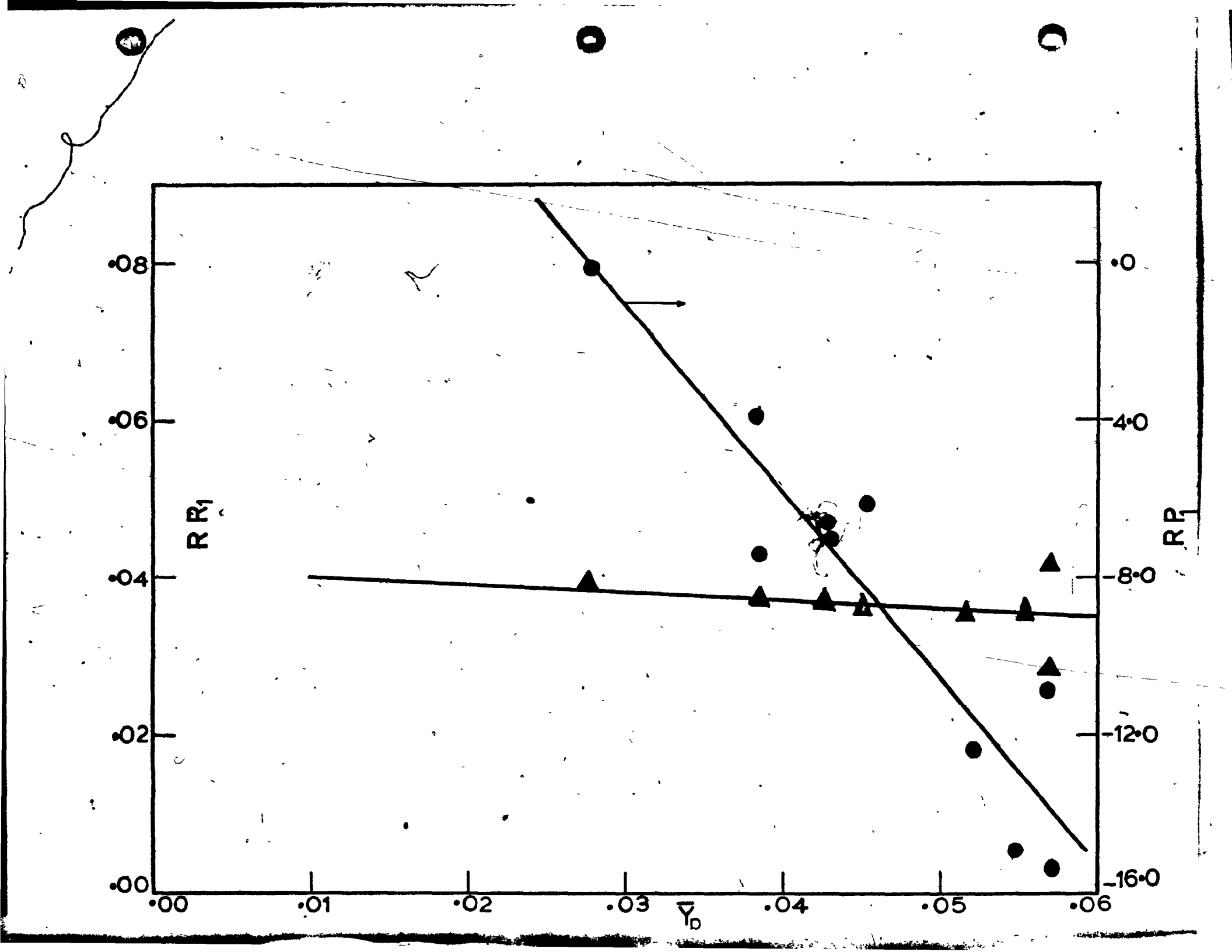
·08
·06
·04
·02
·00
RR1
·0
-4·0
-8·0
-12·0
-16·0
RP1
·00
·01
·02
·03
·04
·05
·06
γD

FIGURE 5-2 RR_2 and RP_2 ($T = 233.5^{o}C$, $h_2 = 0.385$ cm) as a function of propylene gas phase molefraction, $\overline{Y}_p$

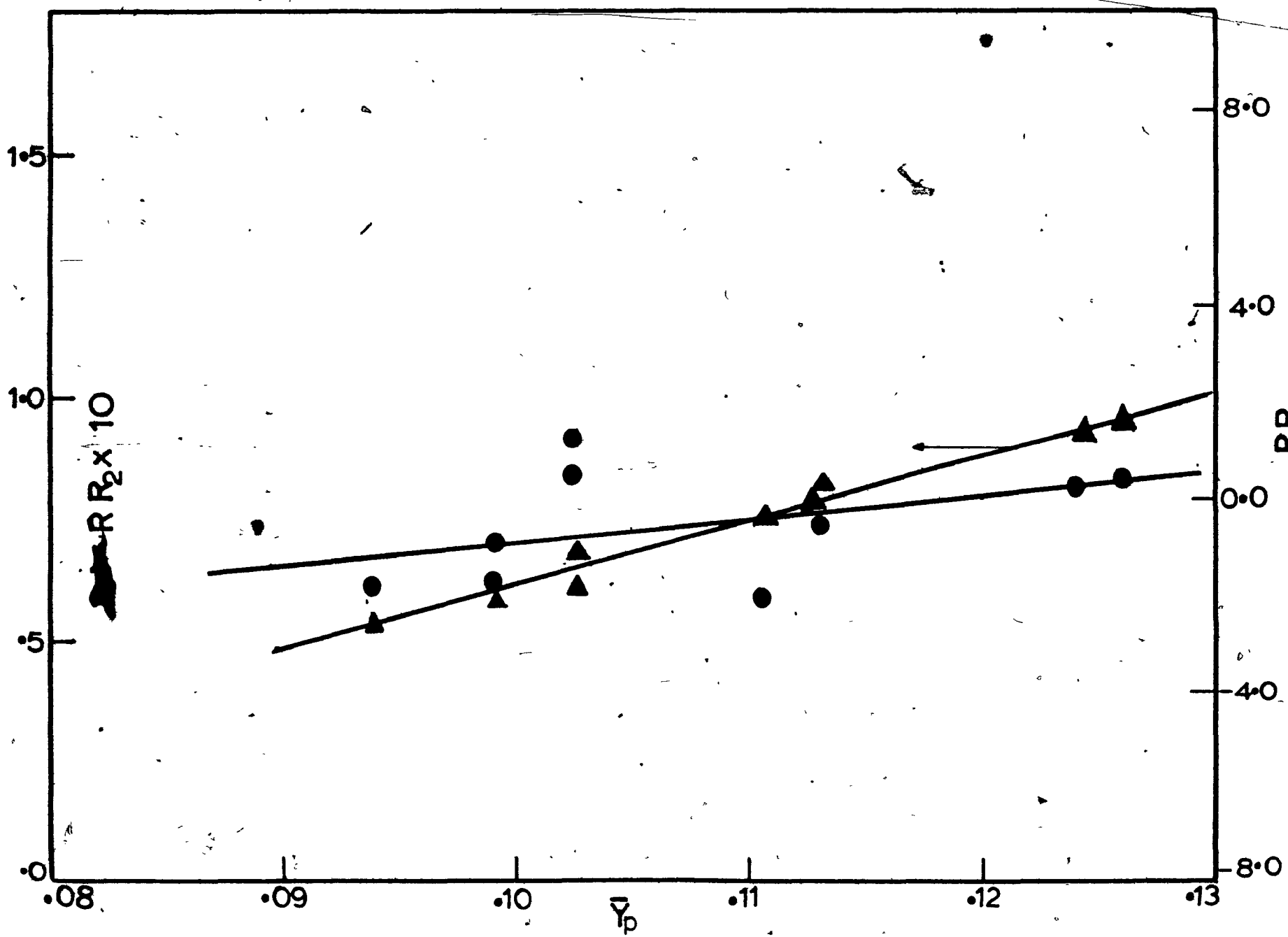
1·5
1·0
·5
·0
R R2 x 10
·08
·09
·10
·11
·12
·13
Yp
8·0
4·0
0·0
4·0
8·0
R R2

FIGURE 5-3 RR_1 and RP_1 ($T = 243.1^{\circ}C$, $h_1 = 0.132$ cm) as a function of propylene gas phase molefraction, $\bar{Y}_p$

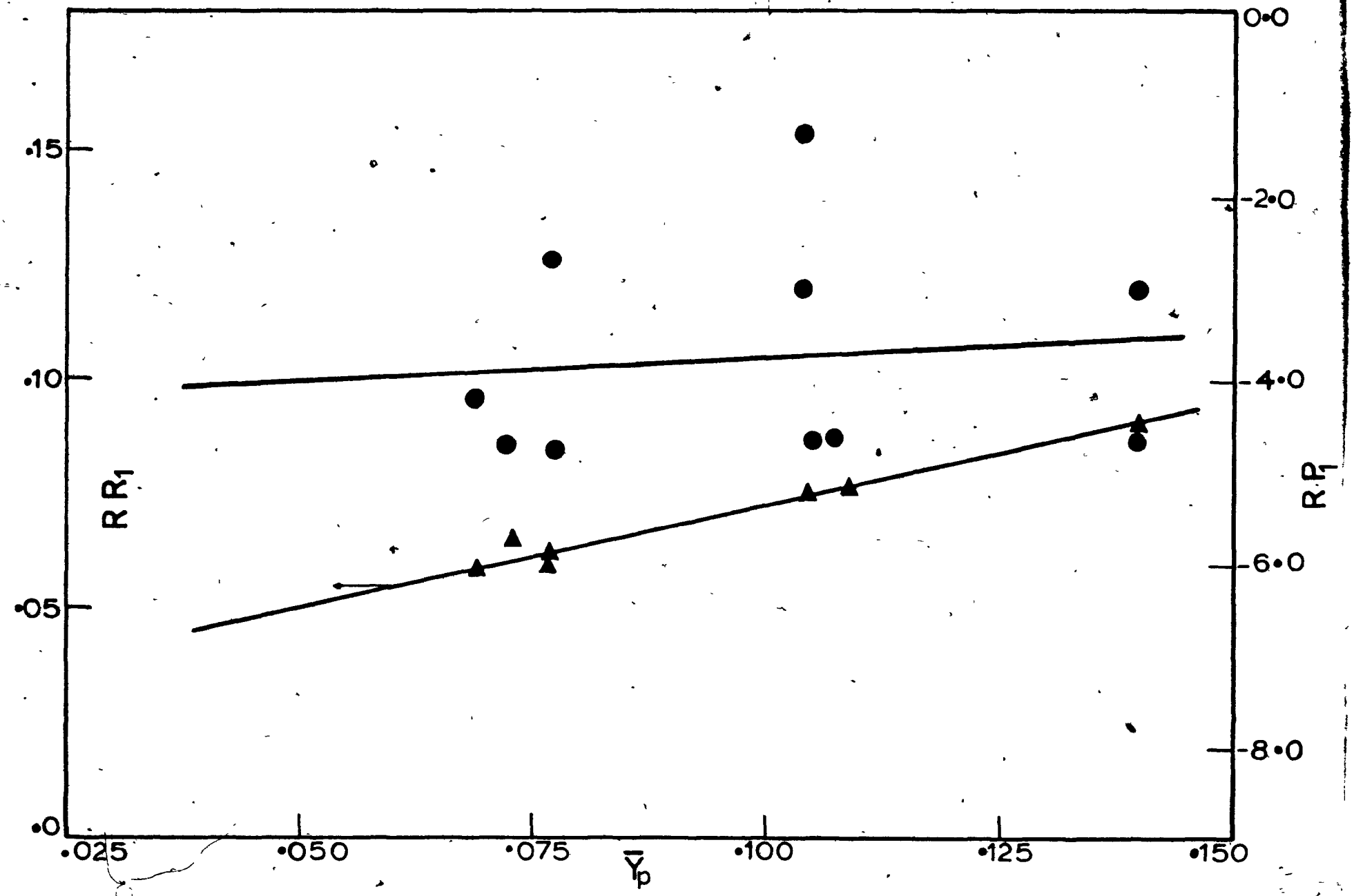
0·0
·15
-2·0
·10
-4·0
R R1
R P1
·05
-6·0
-8·0
·0
·025
·050
·075
·100
·125
·150
Ȳp

FIGURE 5-4 RR_2 and RP_2 ($T = 243.1^{\circ}C$, $h_2 = 0.385$ cm) as a function of propylene gas phase molefraction, $\bar{Y}_p$

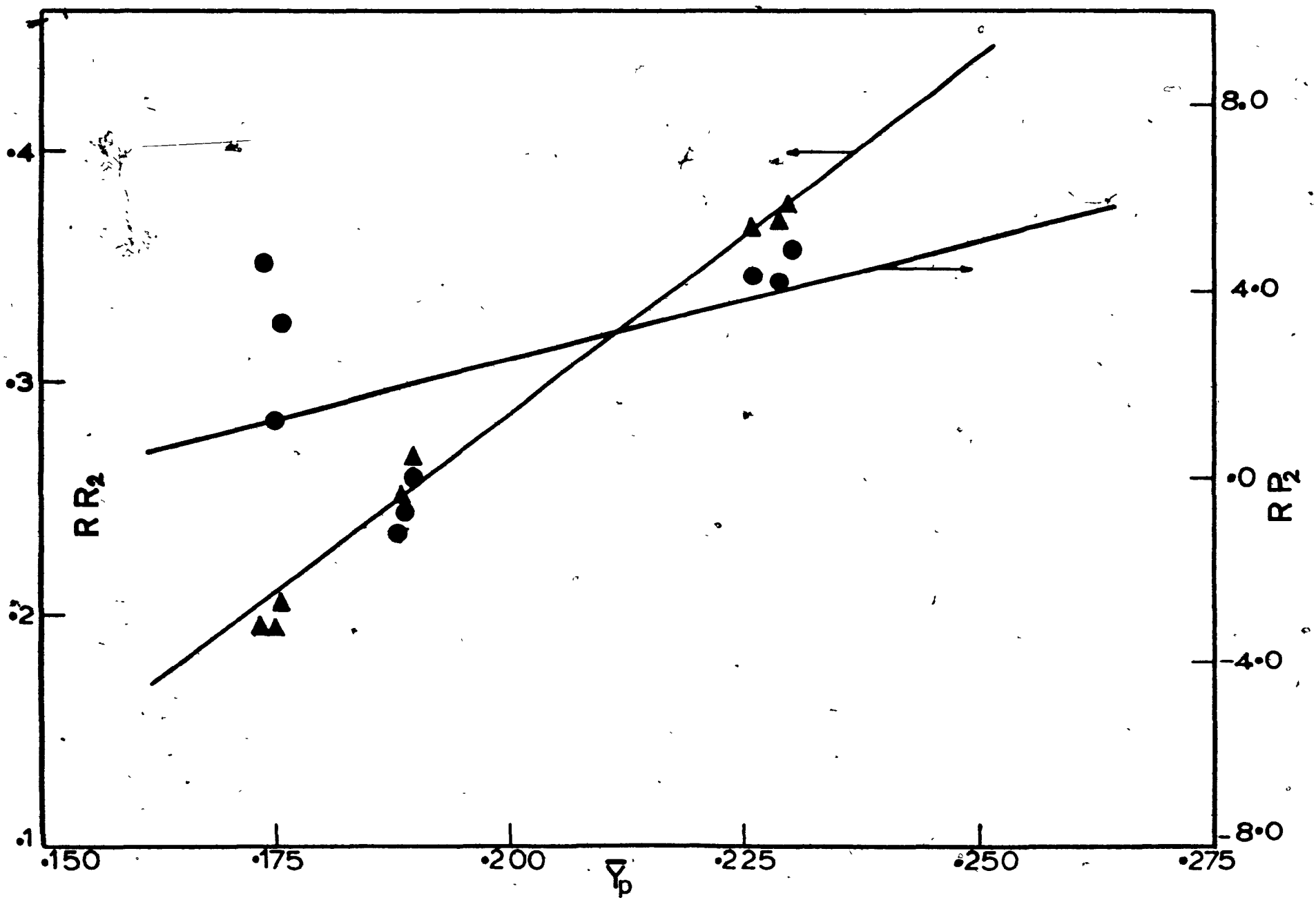
.4
.3
.2
.1
R R2
8.0
4.0
.0
-4.0
-8.0
R R2
.150
.175
.200
.225
.250
.275
γp

FIGURE 5-5 RR_1 and RP_1 ($T = 254.2^{\circ}C$, $h_1 = 0.132$ cm) as a function of propylene gas phase molefraction, $\bar{Y}_p$

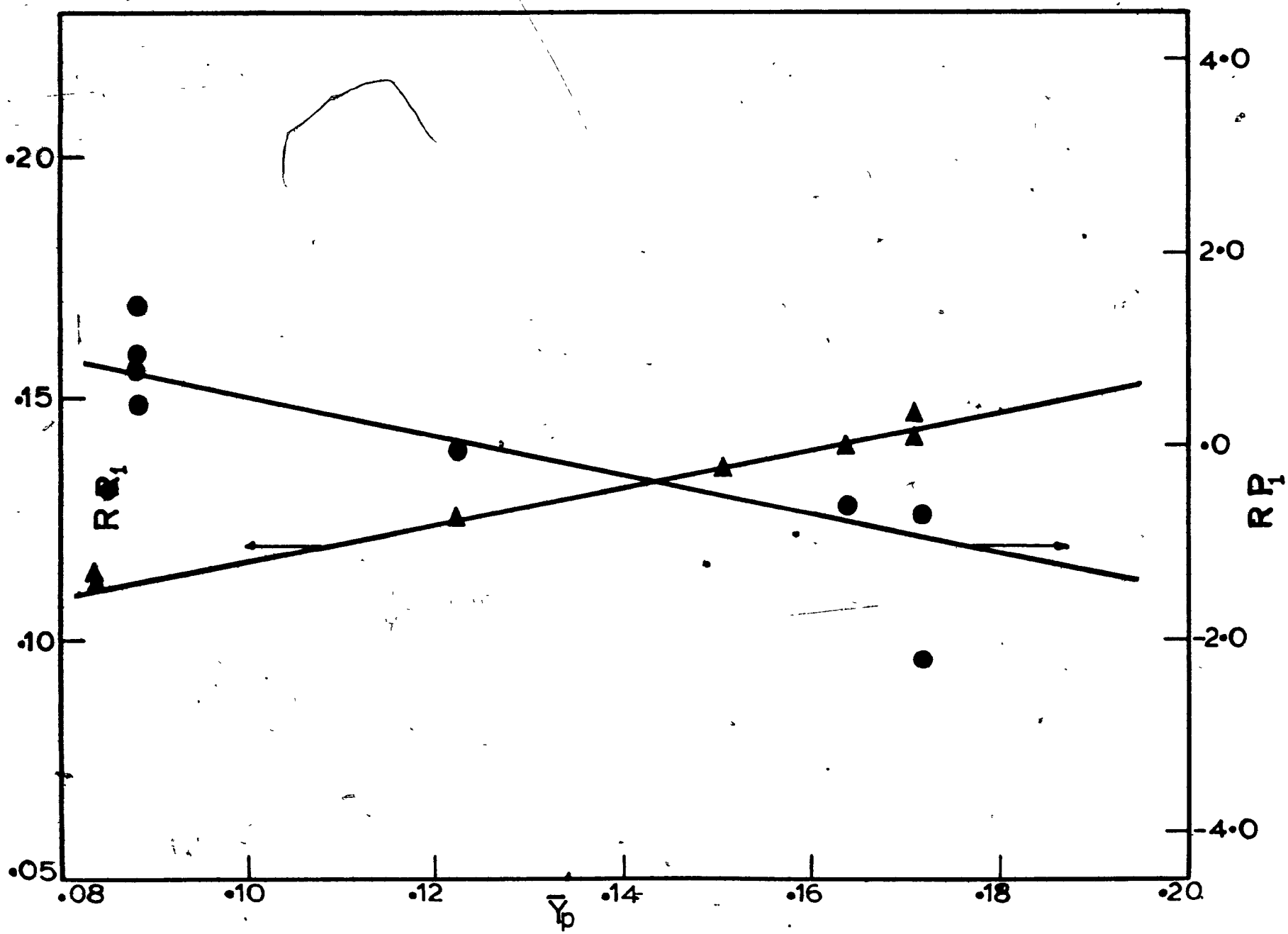
.20
.15
.10
.05
R_1
4.0
2.0
.0
-2.0
-4.0
R_1
.08
.10
.12
.14
.16
.18
.20
$\bar{Y}_p$

FIGURE 5-6 RR_2 and RP_2 ($T = 254.2^{o}C$, $h_2 = 0.385$ cm) as a function of propylene gas phase molefraction, Y_p

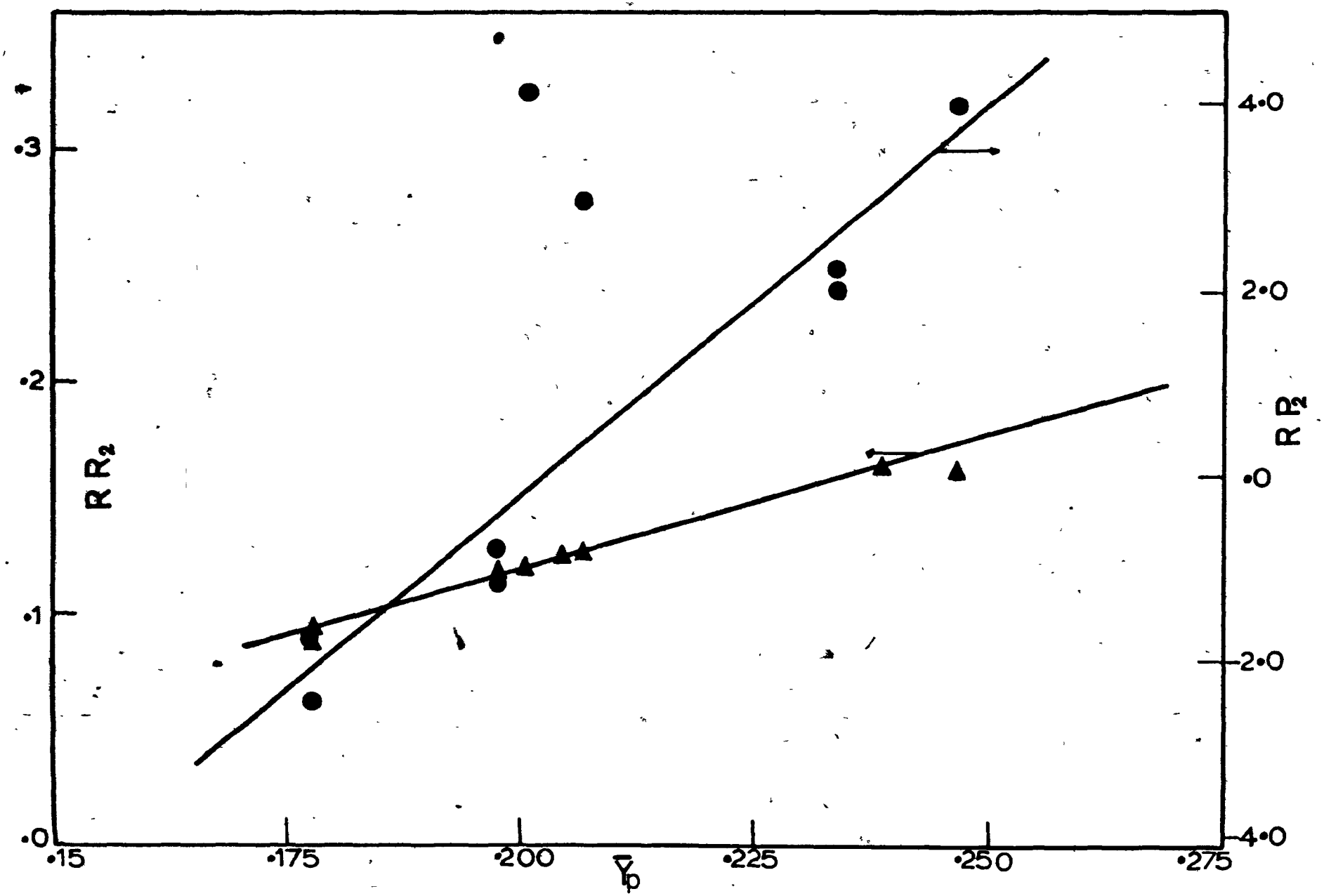
R R2
.3
.2
.1
.0
.15
.175
.200
.225
.250
.275
Vp
4.0
2.0
.0
-2.0
-4.0
R R2

presented in Figures 5-1 to 5-6. The results indicate a linear trend as observed by Kelly (1). Hence a linear least square regression was fitted to the raw experimental data.

The parameter group, RP_i, contains other terms which vary with $\bar{Y}_p$, besides RR_i. These terms are $\hat{\mu}_{1,i}$, the first normalized moment and W_i, the duration of the pulse. Hence RP_i was plotted separately as a function of $\bar{Y}_p$.

The values of RP_i as a function of $\bar{Y}_p$ have also been presented in Figures 5-1 to 5-6. There is severe scatter in these data. This is due to the uncertainty in the values of the experimentally measured first absolute moment, $\mu_{1,i}$. This in turn was caused by the uncertainty of the exact position of the tail of the response curves. A relatively minor change in the tail concentration was enlarged by multiplication with time.

Despite the scatter, the results for the thick pellet at the three temperatures indicate a linear trend. Hence, again, a linear least square regression was fitted to the RP_i parameter groups.

Table 5-1 lists the intercepts and slopes of all fitted straight lines with estimates of their standard deviations. The standard deviations (computed from the sum of squared residuals) of the data about the fitted straight lines are also presented.

Combining the linear regressed values of the parameter groups for both thin and thick pellets at a given $\bar{Y}_p$, Equations 3-31 to 3-46 were solved to estimate the k, D, ψ_Δ and ψ_p parameters. The values of

TABLE 5-1

Linear Regression Coefficients for Parameter Groups as a Function of Reactant Gas Phase Molefraction, Y_p

Average Reaction Temperature	Parameter Group	Intercept	Estimated Standard Deviation	Slope	Estimated Standard Deviation	Standard Deviation About the Line
233.5	RR_1	4.10×10^{-2}	5.55×10^{-3}	-9.98×10^{-2}	1.19×10^{-1}	3.44×10^{-4}
	RR_2	-7.50×10^{-2}	9.98×10^{-3}	1.36	9.99×10^{-2}	3.24×10^{-3}
	RP_1	13.18	3.07	-4.74×10^{2}	6.59x10	1.90
	RP_2	- 5.83	3.77	4.90×10^{1}	3.46x10	1.12
243.1	RR_1	2.83×10^{-2}	2.75×10^{-3}	4.46×10^{-1}	2.68×10^{-2}	2.09×10^{-3}
	RR_2	-9.42×10^{-2}	4.69×10^{-2}	1.07	2.23×10^{-1}	5.23×10^{-3}
	RP_1	- 4.26	5.26	5.20	51.20	1.26
	RP_2	-16.10	1.99	78.80	9.46	7.03×10^{-1}
254.2	RR_1	7.86×10^{-2}	5.16×10^{-3}	3.83×10^{-1}	3.93×10^{-2}	4.29×10^{-3}
	RR_2	-3.28×10^{-1}	1.17×10^{-3}	3.07	2.96×10^{-2}	1.16×10^{-2}
	RP_1	1.52	3.77	- 4.34	28.67	3.12
	RP_2	- 7.69	7.01	51.02	35.29	2.39

TABLE 5-2

Values of the Parameters at an
Average Reaction Temperature of 233.5°C

Gas Phase Propylene Molefraction $\bar{Y}$	Ratio RF_1/RF_2	β cm^{-1}	k $sec^{-1} \times 10^3$	D $cm^2\ sec^{-1} \times 10^4$	ψ_Δ	ψ_p
0.080	1.0087	-	-	-	-	-
0.085	0.8226	8.78	4.596	0.576	6.72	- 61.52
0.090	0.6900	6.27	2.788	0.710	9.40	- 63.53
0.095	0.5908	4.82	1.701	0.731	14.11	- 71.06
0.100	0.5137	3.77	0.996	0.700	22.70	- 84.48
0.105	0.4523	2.89	0.516	0.618	41.85	-113.57
0.110	0.4021	2.06	0.180	0.425	115.48	-217.61
0.115	0.3603	-	-	-	-	-

TABLE 5-3

Values of the Parameters at an Average Reaction Temperature of 243.1°C

Gas Phase Propylene Molefraction $\bar{Y}$	Ratio RF_1/RF_2	β cm^{-1}	k $sec^{-1} \times 10^3$	D $cm^2\ sec^{-1} \times 10^4$	ψ_Δ	ψ_p
0.18	1.1244	-	-	-	-	-
0.20	0.9857	18.683	58.556	1.678	3.66	- 13.73
0.25	0.7813	7.874	13.324	2.149	10.48	- 18.97
0.28	0.7052	6.509	7.178	1.694	20.01	- 28.66
0.30	0.6646	5.878	4.900	1.418	30.29	- 38.71
0.35	0.5850	4.743	1.785	0.793	91.79	- 96.04
0.40	0.5240	3.911	0.260	0.170	701.52	-644.63
0.45	0.4734	-	-	-	-	-

TABLE 5-4

Values of the Parameters at an Average Reaction Temperature of 254.2°C

Gas Phase Propylene Molefraction $\bar{Y}$	Ratio RF_1/RF_2	β cm^{-1}	k $sec^{-1} \times 10^3$	D $cm^2\ sec^{-1} \times 10^4$	ψ_Δ	ψ_p
0.160	0.8433	-	-	-	-	-
0.170	0.7059	6.521	311.51	73.25	0.44	0.19
0.180	0.6048	5.017	48.45	19.25	2.68	- 2.37
0.184	0.5713	4.556	28.78	13.87	4.48	- 4.22
0.186	0.5557	4.344	22.28	11.81	5.77	- 5.52
0.188	0.5409	4.142	17.16	10.00	7.47	- 7.21
0.190	0.5267	3.948	13.05	8.37	9.81	- 9.50
0.192	0.5132	3.762	9.70	6.86	13.17	- 12.75
0.195	0.4939	3.495	5.75	4.71	22.18	- 21.41
0.200	0.4644	3.071	1.11	1.18	114.70	-109.29
0.250	0.2727	-	-	-	-	-

these parameters are presented in Tables 5-2, 5-3 and 5-4.

The solution to Equation 3-36 does not exist for all values of the ratio,

$$\frac{RF_1}{RF_2} = \frac{RR_1F_1/(1-RR_1)}{RR_2F_2/(1-RR_2)} \qquad 5\text{-}51$$

If we now define f, as

$$f(\beta) = \tanh(h_1\beta) - \frac{RF_1}{RF_2}\tanh(h_2\beta) \qquad 5\text{-}52$$

then for the solution of Equation 3-36 to exist, we should have two values of β, β_1 and β_2, such that, for h_2 greater than h_1,

$$f(\beta_1) < 0$$

and

$$f(\beta_2) > 0$$

where

$$\beta_2 > \beta_1 > 0$$

Case 1: β_1

For small positive values of β, (β_1) such that

$$\tanh(h_1\beta_1) \approx h_1\beta_1$$

and

$$\tanh(h_2\beta_1) \approx h_2\beta_1$$

f is given by

$$f(\beta_1) = h_1\beta_1 - \frac{RF_1}{RF_2}h_2\beta_1 < 0$$

and therefore,

$$\frac{RF_1}{RF_2} > \frac{h_1}{h_2}$$

$$= 0.34293 \qquad 5\text{-}53$$

Case 2: β_2

For large values of β, (β_2) such that

$$\tanh(h_1\beta_2) = \tanh(h_2\beta_2) = 1$$

f is given by,

$$f = 1 - \frac{RF_1}{RF_2} > 0$$

Hence,

$$\frac{RF_1}{RF_2} < 1 \qquad 5\text{-}54$$

Therefore for the experiments under consideration in this study, (RF_1/RF_2) should lie within the following ranges, in order that solution to Equation 3-36 may exist:

$$0.34293 < \frac{RF_1}{RF_2} < 1.0 \qquad 5\text{-}55$$

Kelly (1) made the same observation when he solved the zero moment equations for β and γ.

Tables 5-2, 5-3 and 5-4 show the dependency of all parameters on the molefraction of the product Y_p. It can be seen that both the

first order reaction rate constant, k, and the intra-particle diffusion coefficient, D, decrease with increase in $\bar{Y}_p$. The slope of the sorption isotherms of the reactant, ψ_Δ increases with increase in $\bar{Y}_p$. Negative values of the slope of the sorption isotherms of the product were observed and their magnitude increases as $\bar{Y}_p$ increases.

The negative value of the slope of the sorptional isotherm for propylene, ψ_p, can be justified by a more detailed examination of the adsorption phenomena. Let us assume that the adsorption isotherms can be represented in the vicinity of the steady state by Langmuir adsorption equations:

$$C_\Delta = \frac{C_T P_T K_\Delta Y_\Delta}{1+P_T K_\Delta Y_\Delta + P_T K_p Y_p} \qquad 5\text{-}56$$

$$C_p = \frac{C_T P_T K_p Y_p}{1+P_T K_\Delta Y_\Delta + P_T K_p Y_p} \qquad 5\text{-}57$$

For small deviations about the steady state, c_Δ can be given as,

$$c_\Delta = \left(\frac{\partial C_\Delta}{\partial Y_\Delta}\right)_{\bar{Y}_p} y_\Delta + \left(\frac{\partial C_\Delta}{\partial Y_p}\right)_{\bar{Y}_\Delta} y_p$$

$$= \psi_{\Delta\Delta} y_\Delta + \psi_{\Delta p} y_p \qquad 5\text{-}58$$

Therefore, according to Equation 5-56

$$\psi_{\Delta\Delta} = \frac{C_T P_T K_\Delta}{1+P_T K_\Delta Y_\Delta + P_T K_p Y_p} - \frac{C_T P_T^2 K_\Delta^2 Y_\Delta}{(1+P_T K_\Delta Y_\Delta + P_T K_p Y_p)^2} \qquad 5\text{-}59$$

and

$$\psi_{\Delta p} = -\frac{C_T P_T^2 K_\Delta K_p Y_\Delta}{(1+P_T K_\Delta Y_\Delta + P_T K_p Y_p)^2} \qquad 5\text{-}60$$

Similarly,

$$c_p = \psi_{pp} y_p + \psi_{p\Delta} y_\Delta \qquad 5\text{-}61$$

$$\psi_{pp} = \frac{C_T P_T K_p}{1+P_T K_\Delta Y_\Delta + P_T K_p Y_p} - \frac{C_T P_T^2 K_p^2 Y_p}{(1+P_T K_\Delta Y_\Delta + P_T K_p Y_p)^2} \qquad 5\text{-}62$$

and

$$\psi_{p\Delta} = - \frac{C_T P_T^2 K_\Delta K_p Y_p}{(1+P_T K_\Delta Y_\Delta + P_T K_p Y_p)^2} \qquad 5\text{-}63$$

Hence from Equations 5-60 and 5-63,

$$\frac{\psi_{\Delta p}}{\psi_{p\Delta}} = \frac{Y_\Delta}{Y_p} = \eta \qquad 5\text{-}64$$

According to the results of the experiment, η lies between 2.4 and 5.3.

From Equations 5-58 and 5-61, the sum of the deviation values of cyclopropane and propylene concentration is given by,

$$c = (\psi_{\Delta\Delta} + \psi_{p\Delta}) y_\Delta + (\psi_{pp} + \psi_{\Delta p}) y_\Delta \qquad 5\text{-}65$$

Therefore the slopes of the sorption isotherms defined in Equations 3-7a, 3-7b and 3-7c are

$$\psi_\Delta = \psi_{\Delta\Delta} + \psi_{p\Delta} \qquad 5\text{-}66$$

$$\psi_p = \psi_{pp} + \psi_{\Delta p} \qquad 5\text{-}67$$

Hence, from Equation 5-64,

$$\psi_p = \psi_{pp} + \eta \psi_{p\Delta} \qquad 5\text{-}68$$

From Tables 5-2, 5-3 and 5-4 it can be observed that the values of ψ_{pp} and $\psi_{p\Delta}$ are comparable with each other. The multiplication factor,

η, for $\psi_{p\Delta}$ varies from 2.4 to 5.3. Thus the second term $\eta\psi_{p\Delta}$ in Equation 5-68 becomes greater than the first term, ψ_{pp} in magnitude. Moreover, $\eta\psi_{p\Delta}$ is negative, thus resulting in a negative value of ψ_p.

5.2 Sorption Isotherms

Suppose the sorption isotherm for cyclopropane is given by

$$C_\Delta = G_\Delta(Y_\Delta, Y_p) \qquad 5\text{-}69$$

Then,

$$\frac{dC_\Delta}{dY_\Delta} = \frac{\partial G_\Delta}{\partial Y_\Delta} + \frac{\partial G_\Delta}{\partial Y_p}\frac{dY_p}{dY_\Delta} \qquad 5\text{-}70$$

$$= \psi_{\Delta\Delta} + \psi_{\Delta p}\frac{dY_p}{dY_\Delta} \qquad 5\text{-}71$$

$$= \psi_{\Delta\Delta} + \psi_{p\Delta} \cdot \frac{Y_\Delta}{Y_p} \cdot \frac{dY_p}{dY_\Delta} \qquad 5\text{-}72$$

Assuming that,

$$\frac{dY_p}{dY_\Delta} = \frac{y_p}{y_\Delta} \qquad 5\text{-}73$$

where y_p and y_Δ are the small deviations from the steady state values, $\bar{Y}_p$ and $\bar{Y}_\Delta$, the experimental data indicated that,

$$\frac{Y_\Delta}{Y_p}\frac{dY_p}{dY_\Delta} = \frac{\bar{Y}_\Delta}{\bar{Y}_p}\frac{y_p}{y_\Delta} \qquad 5\text{-}74$$

$$\simeq 1$$

$\bar{Y}_\Delta$ is also related to $\bar{Y}_p$ by

$$\bar{Y}_\Delta = \bar{Y}_p\left(\frac{100}{s} - 1\right) \qquad 5\text{-}75$$

where s is the percentage steady state conversion. From the experimental data, s was found to be independent of concentration, hence,

$$\frac{\bar{Y}_\Delta}{\bar{Y}_p} = \frac{d\bar{Y}_\Delta}{d\bar{Y}_p} \qquad 5\text{-}76$$

From these two experimental observations and from Equation 5-72 we can conclude that

$$\frac{dC_\Delta}{dY_\Delta} \simeq \psi_{\Delta\Delta} + \psi_{p\Delta} \qquad 5\text{-}77$$

Hence from Equation 5-66,

$$\frac{dC_\Delta}{dY_\Delta} \simeq \psi_\Delta \qquad 5\text{-}78$$

and, therefore, the binary sorption isotherm for cyclopropane can be obtained from ψ_Δ and $\bar{Y}_\Delta$.

Knowing the slopes of the sorption isotherm of pure propylene at a given temperature where cyclopropane reacts, those of pure cyclopropane could be estimated from Equations 5-64, 5-66 and 5-67. Tables 5-5, 5-6 and 5-7 contain such slopes ($\psi_{\Delta\Delta}$) obtained from the results of the present investigation. The slopes for pure propylene (ψ_{pp}) were extracted from the results of Kelly (1).

The sorption isotherms of 233.5, 243.1 and 254.2 for the pure cyclopropane obtained from the slopes estimated as above are presented in Figure 5-7. The shape of the isotherms indicate possible combination of mono and multi-layer adsorption. Similar types of isotherms were obtained by Kelly (1) working with cyclopropane on 13X zealite pellets at 217°C and by Reyerson and Cameron (60) working with bromine and iodine on silica gel at 137.7°C, 99.9°C, 79°C and 58°C.

TABLE 5-5

Slopes of Sorption Isotherms
Under Reaction Conditions at 233.5°C

Experimental Variables

Temperature	= 233.5	
Pressure	= 750.2	mm Hg
Volumetric Flow Rate, F	= 8.37	$cm^3 sec^{-1}$
Gas Phase Volume, V^+	= 275.41	cm^3
Exposed Area, A	= 101.34	cm^2
Catalyst Thickness, h	= 0.385	cm
Porosity, θ	= 0.50	$(\frac{cm^3 \text{ pore vol.}}{cm^3 \text{ pellet vol.}})$
Percentage Steady State Conversion	= 15.83	%

$\bar{Y}_p$	$\bar{Y}_\Delta$	ψ_Δ	ψ_p	ψ_{pp}	$\psi_{\Delta p}$	$\psi_{p\Delta}$	$\psi_{\Delta\Delta}$
0.085	0.452	6.70	- 61.52	20.50	- 82.02	-15.42	22.13
0.090	0.479	9.40	- 63.57	20.20	- 83.77	-15.75	25.15
0.095	0.505	14.11	- 71.06	20.00	- 91.06	-17.13	31.24
0.100	0.532	22.70	- 84.84	19.80	-104.64	-19.68	42.38
0.105	0.558	41.85	-113.57	19.60	-133.17	-25.05	66.90
0.110	0.585	115.48	-217.61	19.45	-237.06	-44.58	160.06

TABLE 5-6

Slopes of Sorption Isotherms
Under Reaction Conditions at 243.1°C

Experimental Variables

Temperature	= 243.1	°C
Pressure	= 761.8	mm Hg
Volumetric Flow Rate, F	= 8.53	$cm^3 sec^{-1}$
Gas Phase Volume, V^+	= 275.41	cm^3
Exposed Area, A	= 101.34	cm^2
Catalyst Thickness, h	= 0.385	cm
Porosity, θ	= 0.50	
Percentage Steady State Conversion, s	= 29.30	%

Y_p	Y_Δ	ψ_Δ	ψ_p	ψ_{pp}	$\psi_{\Delta p}$	$\psi_{p\Delta}$	$\psi_{\Delta\Delta}$
0.20	0.483	3.66	- 13.73	15.20	- 28.93	- 11.99	15.65
0.25	0.603	10.48	- 18.97	13.20	- 32.17	- 13.33	23.81
0.28	0.676	20.06	- 28.66	12.30	- 40.96	- 16.97	36.98
0.30	0.724	30.29	- 38.71	11.70	- 50.41	- 20.89	51.19
0.33	0.796	57.34	- 64.26	10.90	- 75.16	- 31.15	88.49
0.35	0.845	91.79	- 96.04	10.45	-106.49	- 44.13	135.93
0.37	0.893	161.08	-159.05	10.00	-169.05	- 70.06	231.14
0.40	0.965	701.52	-644.63	9.40	-654.03	-271.05	972.57

TABLE 5-7

Slopes of Sorption Isotherms
Under Reaction Conditions at 254.2°C

Experimental Variables

Temperature	= 254.2	°C
Pressure	= 761.4	mm Hg
Volumetric Flow Rate, F	= 8.66	$cm^3 sec^{-1}$
Gas Phase Volume, V^+	= 275.41	cm^3
Exposed Area, A	= 101.34	cm^2
Catalyst Thickness, h	= 0.385	cm
Porosity, θ	= 0.05	
Percentage Steady State Conversion, s	= 28.6	%

Y_p	Y_Δ	ψ_Δ	ψ_p	ψ_{pp}	$\psi_{\Delta p}$	$\psi_{p\Delta}$	$\psi_{\Delta\Delta}$
0.170	0.424	0.438	0.194	14.6	- 14.41	- 5.77	6.21
0.180	0.449	2.69	- 2.37	14.0	- 16.27	- 6.52	9.20
0.186	0.464	5.77	- 5.52	13.8	- 19.32	- 7.74	11.72
0.190	0.474	9.81	- 9.50	13.6	- 23.10	- 9.25	19.06
0.195	0.484	22.18	- 21.41	13.4	- 34.81	-13.94	36.12
0.200	0.499	114.70	-109.29	13.1	-122.39	-49.02	163.72

FIGURE 5-7 Sorption isotherms of cyclopropane

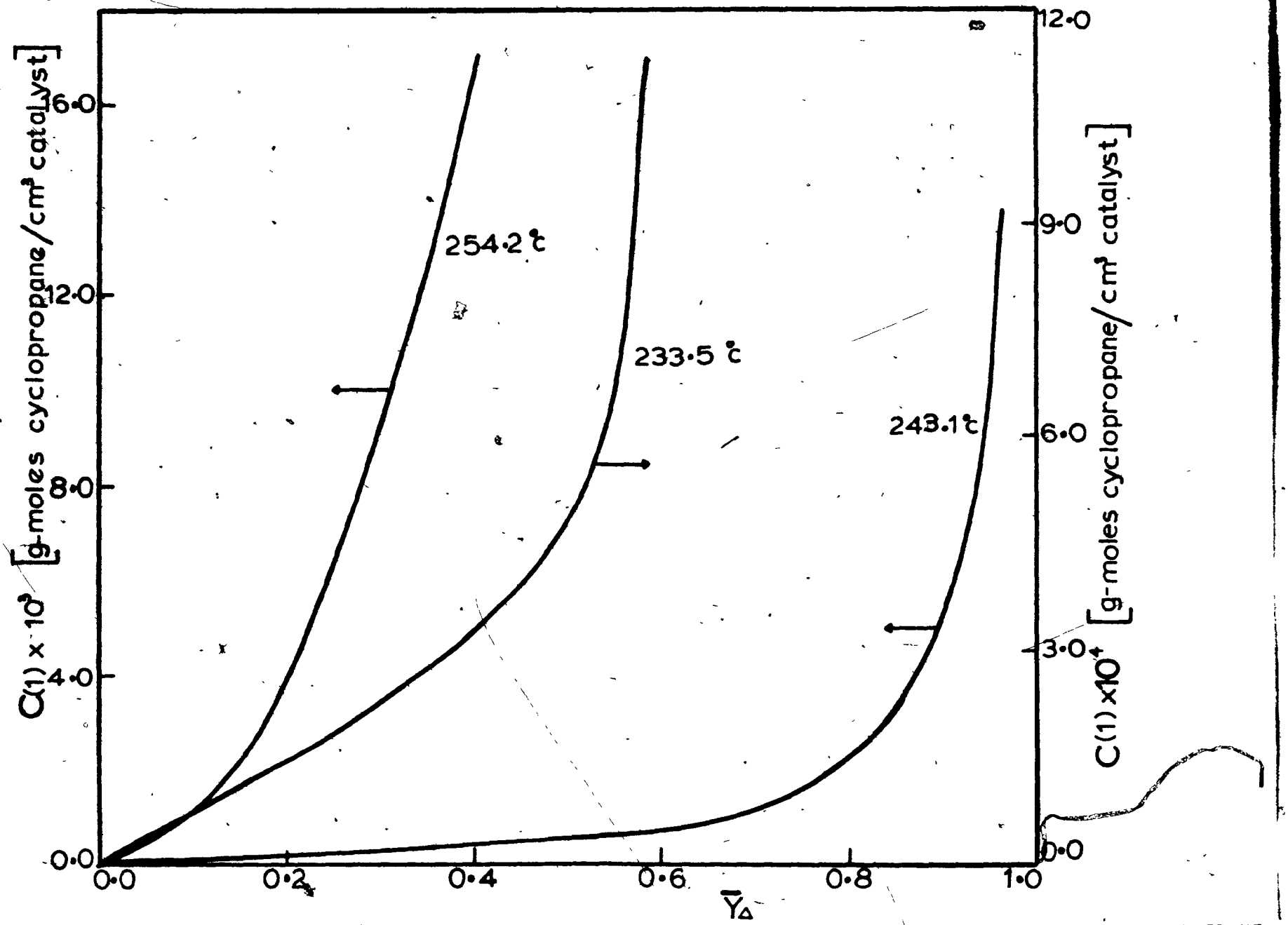
C(1) x 10³ [g-moles cyclopropane/cm³ catalyst]
C(1) x10⁴ [g-moles cyclopropane/cm³ catalyst]
254.2 °c
233.5 °c
243.1 °c
0.0
4.0
8.0
12.0
6.0
9.0
3.0
0.2
0.4
0.6
0.8
1.0
$\bar{Y}_\Delta$

5.3 Integral Average Values of k and D

It is obvious from Tables 5-2, 5-3 and 5-4 that both the first order reaction rate constant k, and the intra-particle diffusivity have a strong dependency on concentration. In order to compare the results of this study with the results previously reported by Kelly (1), the integral average values of these parameters were calculated as follows:

$$\bar{f} = \frac{1}{\bar{Y}_{p_2} - \bar{Y}_{p_1}} \int_{\bar{Y}_{p_1}}^{\bar{Y}_{p_2}} f(\bar{Y}_p) d\bar{Y}_p \qquad 5\text{-}79$$

where f = k or D.

These integral average values for the k and D parameters are presented in Table 5-8. Two temperatures are presented in certain rows of Table 5-8. The first temperature is the average reaction temperature for the present research and the second one is for Kelly's research (1).

Despite the slight difference in temperature at around 252°C, values of the parameters for the two research projects are almost the same. The first order reaction rate constants for the present model gave an activation energy of 31.1 kcal/g-mole. We may compare this value with Kelly's (1) value of 35.7 kcal/g-mole and Habgood and George's (59) value of 40.5 kcal/g-mole.

TABLE 5-8

$\tilde{k}$ and $\tilde{D}$ Values for the Present and Kelly's (30) Model

	Present Model Using Product Concentration		Kelly's (30) Model Using Reactant Concentration	
Temperature °C	$\tilde{D}(cm^2sec^{-1})$ x 10^4	$\tilde{k}(sec^{-1})$ x 10^3	$\tilde{D}(cm^2sec^{-1}$ x 10^4	$\tilde{k}(sec^{-1})$ x 10^3
217.3	-	-	4.1	23
233.5-233.3	0.67	1.65	24.2	9.5
243.1	1.35	11.23	-	-
254.2-251.2	10.21	24.78	11.8	25.3

FIGURE 5-8 Integral average reaction rate constant, k as a function of reciprocal of reaction temperature, $T^{o}K$.

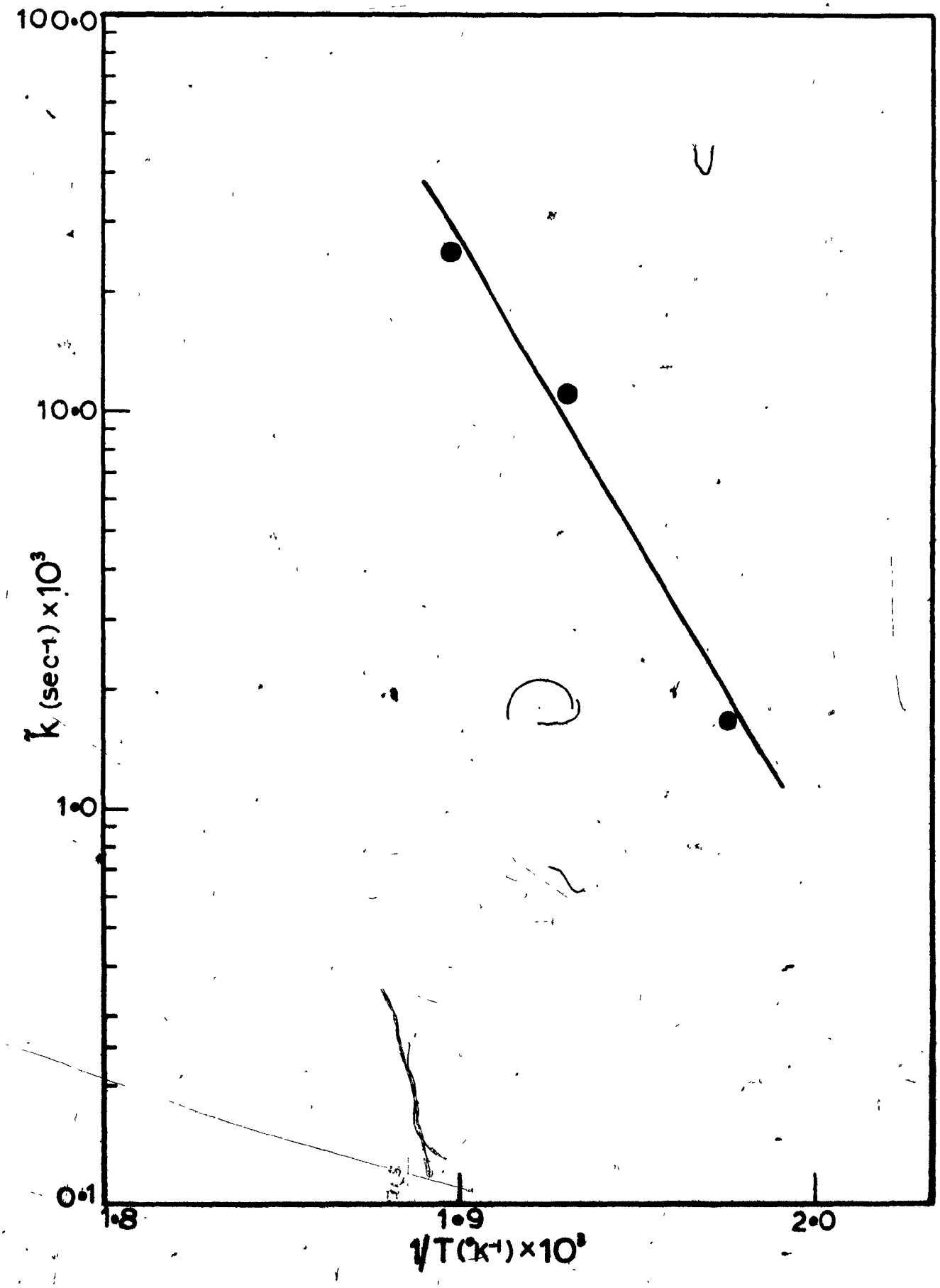
100·0
10·0
1·0
0·1
k (sec⁻¹) × 10³
1·8
1·9
2·0
1/T (°K⁻¹) × 10³

6. DISCUSSION

6.1 Variance Analysis for the Estimated Parameters

As can be seen, the values of the parameters, k, D, ψ_Δ and ψ_p depend on four parameter groups, RR_1, RR_2, RP_1 and RP_2. The variance of k, D, ψ_Δ and ψ_p is then given by

$$\sigma_f^2 = \left(\frac{\partial f}{\partial RR_1}\right)_{RR_2,RP_1,RP_2} \sigma^2_{RP_1} + \left(\frac{\partial f}{\partial RR_2}\right)_{RR_1,RP_1,RP_2} \sigma^2_{RR_2}$$

$$+ \left(\frac{\partial f}{\partial RP_1}\right)_{RR_1,RR_2,RP_2} \sigma^2_{RP_1} + \left(\frac{\partial f}{\partial RP_2}\right)_{RR_1,RR_2,RP_1} \sigma^2_{RP_2} \quad \text{.....5-80}$$

where f = k, D, ψ_Δ or ψ_p.

The partial derivatives of the parameters with respect to the parameter groups can be calculated approximately. This is done by estimating the change in the parameters for a small change in one of the parameter groups about a nominal value while the rest are kept constant as implied by the definition. This is equivalent to a sensitivity test.

Tables 5-8, 5-9 and 5-10 contain the partial derivatives for the k, D, ψ_Δ and ψ_p parameters at the three reaction temperatures. The nominal values about which the partial derivates were estimated are also presented.

From the standard deviations of the parameter groups listed in Table 5-1, the variances of the k, D, ψ_Δ and ψ_p parameters at the average reaction temperature of 233.5°C are given by,

TABLE 5-9

Numerical Approximations to the Partial Derivatives of the k, D, ψ_Δ and ψ_p Parameters with Respect to the Parameter Groups RR_1, RR_2, RP_1, RP_2 at 233.5°C

Temperature = 233.5°C
Percentage Change of the Parameter Group = 1.0%

Nominal Values

Molefraction of Propylene, Y_p	= 0.10
RR_1	= - 3.1999x10^{-2}
RR_2	= 6.1097x10^{-2}
RP_1	= -34.226
RP_2	= - 0.9318
k	= 9.9556x10^{-4}
D	= 7.0049x10^{-5}
ψ_Δ	= 22.704
ψ_p	= -84.841

	Δk	ΔD	$\Delta\psi_\Delta$	$\Delta\psi_p$
ΔRR_1	0.1185	-2.168x10^{-4}	-1700.00	2390.6
ΔRR_2	-0.0683	3.175x10^{-4}	1513.91	1869.1
ΔRP_1	3.383x10^{-5}	2.380x10^{-6}	- 0.778	2.740
ΔRP_2	3.001x10^{-5}	2.102x10^{-6}	0.674	- 1.510

TABLE 5-10

Numerical Approximations to the Partial Derivatives of the k, D, ψ_Δ and ψ_p Parameters with Respect to the Parameter Groups RR_1, RR_2, RP_1, and RP_2 at 243.1°C

Temperature = 243.1°C
Percentage Change in the Parameter Group = 1.0%

Nominal Values

Molefraction of Propylene, $\bar{Y}_p$	= 0.30
RR_1	= 0.1620
RR_2	= 0.2270
RP_1	= -2.6953
RP_2	= 7.5419
k , sec^{-1}	= 4.8988×10^{-3}
D , $cm^2 sec^{-1}$	= 1.4177×10^{-4}
ψ_Δ	= 30.294
ψ_p	= -38.710

	Δk	ΔD	$\Delta\psi_\Delta$	$\Delta\psi_p$
ΔRR_1	0.1347	2.778×10^{-4}	-467.3	527.8
ΔRR_2	-0.1066	-4.449×10^{-4}	600.0	-544.1
ΔRP_1	4.758×10^{-4}	1.413×10^{-5}	-2.9368	4.535
ΔRP_2	-4.748×10^{-4}	-1.379×10^{-5}	2.958	- 3.515

TABLE 5-11

Numerical Approximations of the Partial Derivatives of the k, D, ψ_Δ and ψ_p Parameters with Respect to the Parameter Groups RR_1, RR_2, RP_1 and RP_2 at 254.2°C

Temperature = 254.2°C
Percentage Change in the Parameter Group = 1.0%

Nominal Values

Molefraction of Propylene, $\bar{Y}_p$	= 0.185
RR_1	= 0.1495
RR_2	= 0.2409
RP_1	= 0.7172
RP_2	= 1.7529
k	= 2.5329×10^{-2}
D	= 1.2801×10^{-3}
ψ_Δ	= 5.0825
ψ_p	= -4.8321

	Δk	ΔD	$\Delta\psi_\Delta$	$\Delta\psi_p$
ΔRR_1	1.121	2.080	-160.4	174.5
ΔRR_2	-0.8195	-1.860×10^{-2}	168.2	-161.9
ΔRP_1	2.455×10^{-2}	1.255×10^{-3}	-4.099	6.360
ΔRP_2	-2.411×10^{-2}	-1.217×10^{-3}	4.914	- 5.371

$$\sigma_k^2 = 1.662\times10^{-9} + 4.897\times10^{-8} + 4.132\times10^{-9} + 1.130\times10^{-9}$$
$$= 5.589\times10^{-8} \quad \text{.....5-81}$$

$$\sigma_D^2 = 5.665\times10^{-15} + 1.058\times10^{-12} + 2.045\times10^{-11} + 5.542\times10^{-12}$$
$$= 2.70\times10^{-11} \quad \text{.....5-82}$$

$$\sigma_{\psi_\Delta}^2 = 0.342 + 24.050 + 2.185 + 0.5698 = 27.16 \quad \text{5-83}$$

$$\sigma_{\psi_p}^2 = 0.676 + 36.670 + 27.102 + 2.860 = 40.21 \quad \text{5.84}$$

Similarly, the variances for the parameters at 243.1°C are given by

$$\sigma_k^2 = 7.93\times10^{-8} + 3.108\times10^{-7} + 3.59\times10^{-7} + 1.11\times10^{-7}$$
$$= 8.60\times10^{-7} \quad \text{.....5-85}$$

$$\sigma_D^2 = 3.37\times10^{-13} + 8.65\times10^{-13} + 3.17\times10^{-10} + 9.40\times10^{-11}$$
$$= 4.12\times10^{-10} \quad \text{.....5-86}$$

$$\sigma_{\psi_\Delta}^2 = .95 + 9.85 + 13.69 + 4.32 = 27.81 \quad \text{5-87}$$

$$\sigma_{\psi_p}^2 = 1.21 + 8.10 + 32.65 + 70.57 = 121.53 \quad \text{5-88}$$

At 254.2 the variances for the parameters are obtained as follows

$$\sigma_k^2 = 2.31\times10^{-5} + 9.04\times10^{-6} + 5.87\times10^{-3} + 3.32\times10^{-3}$$
$$= 9.22\times10^{-3} \quad \text{.....5.89}$$

$$\sigma_D^2 = 7.96\times10^{-5} + 4.66\times10^{-8} + 1.53\times10^{-5} + 8.46\times10^{-6}$$
$$= 10.34\times10^{-5} \quad \text{.....5-90}$$

$$\sigma_{\psi_\Delta}^2 = 0.474 + 3.81 + 163.56 + 137.93 = 305.80 \quad \text{5-91}$$

$$\sigma_{\psi_p}^2 = 0.749 + 3.53 + 393.75 + 164.78 = 562.71 \quad \text{5-92}$$

TABLE 5-12

Nominal Values of k, D, ψ_Δ and ψ_p
Parameters with their Approximate Standard Deviations

Average Temperature °C	Parameters	k sec^{-1} 10^3	D $cm^2 sec^{-1}$ 10^4	ψ_Δ	ψ_p
233.5	Nominal Values	0.996	0.700	22.70	-84.84
	Approximate Standard Deviations	0.24	0.052	5.21	6.34
243.1	Nominal Values	4.9	1.42	30.29	-38.71
	Approximate Standard Deviations	0.93	0.20	5.27	10.61
254.2	Nominal Values	25.33	12.80	5.08	- 4.8
	Approximate Standard Deviations	96.03	101.68	17.49	23.72

It is evident from Tables 5-8, 5-9, and 5-10 that the values of the parameters k, D, ψ_Δ and ψ_p are more sensitive to the RR_i group parameters than RP_i. However, because of the appreciable scatter in the experimental data of RP_i group parameters, they have larger standard deviations than RR_i group parameters as indicated by Table 5-1. Therefore, it is not surprising that Equations 5-81 to 5-92 indicate almost equal contribution from all the parameter groups to the variances of the parameters. Even Equations 5-86 to 5-89, 5-91 and 5-92 indicate that RP_i parameter groups contribute more to the variances of the parameter than RR_i parameter groups, contrary to the observation of Kelly (1).

According to Table 5-12 the results at 233.5°C and 243.1°C indicate low standard deviations compared to the nominal values. In all cases, the standard deviation is less than 30 per cent of the nominal values. On the other hand the results at 254.2°C show that the standard deviations are multiples of the nominal values. This was caused by the large scatter of the experimental data for the parameter groups. With respect to the RR_i parameter groups, the standard deviations of the fitted lines at 254.2°C are about 10 times the standard deviations at the other average reaction temperatures.

6.2 Variation in the Estimated Parameters

Contrary to expectation, the estimated first-order reaction rate constant, k, and the intra-particle diffusivity vary with concentration. This deviation from the hypothesis underlying the development of the mathematical model can be attributed to a number of factors. With

respect to the reaction rate constant, k, its variation with concentration can be attributed to the fact that the reaction rate may not be first order. It is possible that the reaction goes through a series of steps which results in a non-first order reaction rate. It is possible that the product, propylene, underwent a significant amount of further reaction such as dimerization. Hence the concentration of propylene was underestimated.

There is no particular reason to expect D to be independent of concentration. However, the model is followed fairly well at lower temperatures, but not at 254°C. Possibly this is caused by the increased rate of dimerization at high temperatures.

In developing the mathematical model it was assumed that the concentration deviation was negligible compared to the steady state value. However, the sensitivity of the concentration detector was not high enough to allow a deviation concentration to be small. A sample of the program output presented in the Appendix indicates a maximum concentration deviation of about 11 per cent of the steady state value. Thus the concentration deviation is not negligible compared to the steady state value. This could account for the variation of k, D with concentration.

There was considerable scatter in the raw experimental data and this definitely affected the values of the estimated parameters.

In the mathematical model it was assumed that the external mass transfer resistance is negligible compared with the diffusional and reaction resistance. This is not strictly true. The surface of the

pellets were not in line with the top of the die holes and this could result in significant interfacial mass transfer resistance. A slight crack between a pellet and the reactor could permit a leakage flux between the bulk gas phase and the vertical side of the pellet. This would have the effect of systematic errors in A and h, but the contribution is probably small and, in any case, it is nearly constant for all of the experiments.

7. CONCLUSION

A mathematical model based on the concentration of the product for the estimation of the parameters characterizing heterogeneous catalysis had been developed. The parameters are the first-order reaction rate constant, diffusion coefficient and the slopes of the sorption isotherms for the product and the reactant.

The mathematical model was tested with a continuous stirred volume catalytic reactor (gradientless) using the pulse response technique. The reaction was the isomerization of cyclopropane to propylene on 13X zeolite catalyst.

Kelly (1) performed the same experiment. However, in basing the mathematical model on the reactant concentration he could estimate only three parameters, namely the first-order reaction rate constant, diffusion coefficient and the slope of the sorptional isotherm for the reactant.

The estimated first-order reaction rate constant, k, and the diffusion coefficient, D, varied with concentration. However the integral average values of these parameters can be compared with those reported by Kelly (1). At the average reaction temperature around 252°C, $\bar{k}$ and $\bar{D}$ compare very favourably (Table 5-8).

With the present mathematical model, the slopes of the binary sorption isotherms for both the reactant and the product had been determined simultaneously. It had been observed that the slope of the

binary sorption isotherm for the product (propylene), which is less selectively adsorbed than the reactant (cyclopropane) by the 13X zealite catalyst (1), was negative. This observation can be explained assuming the Langmuir-Hinshelwood sorption isotherms in the vicinity of the steady state.

Knowing the slopes of the sorption isotherm of the product (and assuming the Langmuir-Hinshelwood sorption isotherms), those of the reactant could be estimated from the mathematical model developed. The shape of the sorption isotherm indicates a combination of mono- and multi-layer adsorption.

Within the limits of the accuracy of the concentration detector and assuming that there is no sorption of nitrogen at the reaction temperature, it can be concluded from the experimental results that the steady state conversion of the reactant is independent of the reactant inlet concentration to the reactor.

The results of the present investigation indicate considerable improvement in the degree of certainty in the experimentally measured moment zero-moment as compared to the results of Kelly (1). The parameters were very sensitive to the parameter groups involving only the zero-moment (RR_i). However, this was cancelled out by the small standard deviations of the linear regressed lines fitted to the raw experimental data.

There was large scatter of the parameter groups involving the first normalized moment (RP_i). This was also cancelled out by the low

sensitivity of the parameters to these parameter groups. Thus the variance analysis indicated equal contribution to the variance of the parameters from all the parameter groups.

In developing the mathematical model, it was assumed that the concentration deviation about the steady state value was negligible compared to the steady state value. But in order that the deviation concentration could be monitored, it had to be large enough. This demanded that the molefraction of the reactant in the inlet gas be pulsed by 0.2 for the thin pellet and 0.1 for the thick pellet when generating the square wave. A sample of the program output has been presented in the Appendix. It indicates a maximum concentration deviation of about 11 per cent of the steady state value. Thus the concentration deviation is not negligible compared to the steady state value. This could account for the variation of the estimated parameters with concentration.

The most effective way to eliminate this constraint is to use a more sensitive concentration detector so that the deviation could be made as small as possible.

REFERENCES

1. Kelly, J.F., Thesis "Parameter Estimation in Heterogeneous Catalysis", McGill University (1975).
2. Kokes, R.J., Tobin, H. Jr. and Emmett, P.H., J. Am. Chem. Soc. 77, 5860 (1955).
3. Hall, W.K. and Emmett, P.H., J. Am. Chem. Soc. 79, 2091 (1957).
4. Hall, W.K., MacIver, D.S. and Weber, H.P., Ind. Eng. Chem. 52, 421 (1960).
5. Greene, S.A. and Pust, H., Anal. Chem. 30, 1039 (1958).
6. Tamaru, K., Nature 183, 319 (1959).
7. Nakanishi, J. and Tamaru, K., Trans. Faraday Soc. 59, 1470 (1963).
8. Bassett, D.W. and Habgood, H.W., J. Phys. Chem. 64, 769 (1960).
9. Kubin, M., Collr. Czech. Chem. Commun. 30, 1104, 2900 (1965).
10. Kucera, E., J. Chromatography 19, 237 (1965).
11. Masamune, S. and Smith, J.M., AIChE Journal 11, 34, 41 (1965).
12. Schneider, P. and Smith, J.M., ibid 14, 886 (1968).
13. Padberg, G. and Smith, J.M., J. Catalysis 12, 172 (1968).
14. Adrian, J.C. and Smith, J.M., ibid 18, 57 (1970).
15. Suzuki, M. and Smith, J.M., ibid 21, 336 (1971).
16. Suzuki, M. and Smith, J.M., ibid 23, 321 (1971).
17. Cerro, R.L. and Smith, J.M., ibid, Ind. Eng. Chem. Fund. 8, 796 (1970).
18. Hashinioto, M. and Smith, J.M., Ind. Eng. Chem. Fund. 12, 353 (1973).
19. Kawazoe, K., Suzuki, M. and Chihara, K., J. Chem. Eng. Japan 1, 32 (1968).
20. Richardson, J.T., Freidrich, H. and McGill, R.H., J. Catal. 37, 1 (1975).

21. Richardson, J.T., Freidrich, H. and McGill, R.H., J. Catal. 37, 8 (1975).

22. Balder, J.R. and Petersen, E.E., J. Catalysis 11, 195, 202 (1968).

23. Gibilaro, L.G., Gioia, F. and Greco, G. Jr., The Chem. Eng. Journal 1, 85 (1970).

24. Suzuki, M. and Smith, J.M., AIChE Journal 18, 326 (1972).

25. Dogu, G. and Smith, J.M., AIChE Journal 21, 1, p.58 (1975).

26. Bennett, C.O., AIChE Journal 13, 890 (1967).

27. Bennett, C.O., Cutlip, M.B. and Yang, C.C., Chem. Eng. Sci., 27, 2255 (1972).

28. Cutlip, M.B., Yang, C.C. and Bennett, C.O., AIChE Journal 18, 1073 (1972).

29. Relyea, D.L. and Perlmutter, D.D., Ind. Eng. Chem. PDD 7, 261 (1968).

30. Kelly, J.F. and Fuller, O.M., Can. J. Chem. Eng. 50, 534 (1972).

31. Rosen, J.B., J. Chem. Phys. 20, 387 (1952).

32. Rosen, J.B., Ind. Eng. Chem. 46, 1590 (1954).

33. Edeskuty, F.J. and Amundson, N.R., J. Phys. Chem. 56, 148 (1952).

34. Kawazoe, K. et al, J. Chem. Eng. Japan 7, 3, p.158 (1974).

35. Suzuki, M. and Kawazoe, K., J. Chem. Eng. Japan, 7, 5, p.346 (1974).

36. Kocirik, M., J. Chromotography 30, 459 (1967).

37. Roginskii, S.Z. and Rozental, A.L., Kinet Katal 5, 104 (1964).

38. Donisova, T.A. and Rozental, A.L., ibid, 8, 441 (1967).

39. Suzuki, M. and Smith, J.M., Chem. Eng. Sci. 26, 221 (1971).

40. Langer, S.H., Yurchak, J.Y. and Patton, J.E., Ind. Eng. Chem. 61, 4, p.10 (1969).

41. Suzuki, M., J. Chem. Eng. Japan, 6, 6, p.540.

42. Schneider, P. and Smith, J.M., AIChE Journal 14, 762 (1968).

43. Eberly, P.E. Jr., I. and E.C. Fund. 8, 25 (1969).

44. Tamaru, K., Advances in Catalysis, 15, p.25.

45. Cunningham, R.E. and Smith, J.M., AIChE Journal 9, 3, p.419 (1963).

46. Otani, S. and Smith, J.M., J. Catalysis 5, p.332 (1966).

47. Kasaoka, S., Sakata, Y. and Nitta, K., J. Chem. Eng. Japan 1, p.32 (1968).

48. Satterfield, C.H. and Cadle, P.J., I. and E.C. Fund. 1, 2, p.203 (1968).

49. Thomas, H.C., J. Chem. Phys. 19, 1213.

50. Kubota, H. and Yamanka, Y., J. Chem. Eng. Japan 2, 238.

51. Brown, L.F., Haynes, H.W. and Manogue, W.H., J. Catalysis 14, p.220 (1969).

52. Wakao, N., J. Chem. Eng. Japan, 3, 1, p.9 (1970).

53. Mitani, M. and Hamai, S., J. Chem. Eng. Japan, 5, 4, p.364 (1927).

54. Riekert, L., Advances in Catalysis 21, p.281 (1970).

55. Kumazawa, H. and Morita, M., J. Chem. Eng. Japan 5, 4, p.375 (1972).

56. Neale, G.H. and Nader, W.K., AIChE Journal 19, 1, p.112 (1973).

57. Toei, R. et al, J. Chem. Eng. Japan 6, 1, 50 (1973).

58. Jacobs, P.A. and Heylen, C.F., J. Catalysis 34, p.267 (1974).

59. Habgood, H.W. and George, Z.M., Proc. Soc. Chem. Eng. Conf. on Molecular Sieves, London, 130 (1968).

60. Reyerson, L.H. and Cameron, A.E. J. Phys., Chem., 39, p.181 (1958).

APPENDIX A

FIGURE A-1 Programme listings for the estimation of the parameter groups from the raw experimental data, and a sample output.

```
C     NUMBER OF DATA POINTS (RESPONSE)
C     BIFUNCTIONARY PULSING ON DETECTOR WITH NO ABSORBING SAMPLE PRESENT
C     PERTURBATION (MM-HG)
C     TEMPERATURE (DEGREES K)
C     JEDPR= RUN CARD NUMBER
C     E(J) = ENERGY PULSE ON THE REACTOR WITH ABSORBING SAMPLE PRESENT
C     RMOLF(J)= MOLE FRACTION OF COMPONENT PULSED IN REACTOR RESPONSE
C     TIM(J)= TIME(RESPONSE)
C     ABSIN(J)=LN(A/A(J))
C     PA(J)= PARTIAL PRESSURE
C     CONC(J)= CONCENTRATION
C     R(J)= CONCENTRATION * TIME
C     M(J) IS A GENERATED FUNCTION
C     SUBJU REPRESENTS THE FUNCTION SUBROUTINE THAT
C     CALCULATES THE INTEGRAL OF A GENERATED FUNCTION
C     U0 AND U1 ARE THE NORMALIZED 1ST AND 2ND MOMENTS
C     UV1 IS THE NORMALIZED 1ST MOMENT
C     IRO THE NUMBER OF COMPLETE RUNS TO BE ANALYZED
C     CCO= STEADY STATE CONCENTRATION
C     SCONV= STEADY STATE CONVERSION
C     TCONV= TRANSIENT STATE CONVERSION
C     FLOW= VOLUMETRIC GAS FLOWRATE
C     VPLUG= VOLUME OF GAS PHASE
C     AREA= TOTAL SURFACE AREA OF PELLET
C     L= THICKNESS OF PELLET
0001          IMPLICIT REAL*8(A-H,L,O-Z),INTEGER(I-K,N-N)
0002          DIMENSION RMOLF(100),E(100),ABSIN(100),PA(100),CONC(100),TIM(100)
             1,R(100),M(100),XMOLPR(100),PAR(100),CONCR(100),RM(100),RR(100),RP(
             2100),CC(100),RG(100),RP(100),V(100)
0003          READ(5,1000
0004          READ(5,11)JR
0005       11 FORMAT(I2)
0006          DO 1000 JOVER=1,JR
0007          READ (5,111)ER
0008          READ (5,12) R/ZERO
0009       12 FORMAT(D12.5)
0010          READ(5,102)A,B,C
0011          READ(5,102)VPLUG,AREA,L,THETA
0012      102 FORMAT(4D10.5)
0013          READ (5,103) PRESS,TEMP
0014          WRITE(6,99)
0015          WRITE(6,97)
0016          WRITE(6,98) VPLUG
0017          WRITE(6,97)
0018          WRITE(6,91) AREA
0019          WRITE(6,97)
0020          WRITE(6,92) L
0021          WRITE(6,97)
0022          WRITE(6,93) THETA
0023          WRITE(6,97)
0024          WRITE(6,94) PRESS
0025          WRITE(6,97)
0026          WRITE(6,95) TEMP
0027          WRITE(6,97)
```

4328-43

```
0000                  WRITE(6,98) A
0100                  WRITE(6,97)
0110                  WRITE(6,97) B
1111                  WRITE(6,97)
1112                  WRITE(6,98) C
0113                  WRITE(6,97)
1114                  WRITE(6,99) DEPTH
1115                  WRITE(6,97)
0116                  WRITE(6,98)
1117              40  FORMAT('1',/////////,'SIR JOHN')
1118              41  FORMAT('0',BX,'NUMBER OF FLUXES',I2,'.',BX,'01')
0119              42  FORMAT('0',BX,'AREA',12X,'01',F12.8,BX,'01')
0120              43  FORMAT('0',BX,'MOLE',BX,'01',D12.8,BX,'01')
1121              44  FORMAT('0',BX,'ENTROPY',D12.8,BX,'01')
0122              45  FORMAT('0',BX,'ENTHALPY',D12.8,BX,'01')
0123              46  FORMAT('0',BX,'TEMP',12X,'01',D12.8,BX,'01')
0124              47  FORMAT('0',BX,'MW',BX,'01',D12.8,BX,'01')
0125              48  FORMAT('0',BX,'MF',BX,'01',D12.8,BX,'01')
0126              49  FORMAT('0',BX,'MF/MW',D12.8,BX,'01')
0127              50  FORMAT('0',BX,I10)
0128                  DO 100 K= 1,10
0129                  READ(5,99) JCODA
0130                  READ (5,101) SCALEP,TIMEP
0131              99  FORMAT(I3)
0132                  READ(5,7) N
0133              7   FORMAT(I10)
0134                  READ(5,102) FLUX
0135                  READ(5,102) W
0136                  READ(5,102) EOUT
0137                  READ(5,102) XMOLIN,XMOBP
0138                  DO 8 J=1,N
0139                  READ(5,102) P(J), TIME(J)
0140                  P(J)= EOUTOR(J)*SCALEP
0141                  TIME(J)= TIME(J)*TIMEP
0142              8   CONTINUE
0143                  WRITE (6,40)
0144                  WRITE(6,41)
0145                  WRITE(6,42)
0146                  WRITE(6,99)JCODA
0147                  WRITE(6,43)
0148                  WRITE(6,41)
0149                  WRITE(6,44)
0150                  WRITE(6,42)
0151                  WRITE(6,44)
0152                  WRITE(6,41)
0153                  WRITE(6,45)
0154                  WRITE(6,43)
0155                  WRITE(6,44)
0156                  WRITE(6,41)
0157                  WRITE(6,46)
0158                  DO 17 J=1,N
0159                  ABSOR(J)=LOG(EZERO/P(J))
0160                  XMOLE(J) = A*P**ABSOR(J) * COABSOR(J)*ABSOR(J)
```

```
                PA(J) = RMOLE(J)*PRESS
                CONC(J) = PA(J)/R/TEMP
                WRITE(6,44) TIME(J),DT(J),RMOLE(J),PA(J),CONC(J)
             10 CONTINUE
                WRITE(6,46)
                WRITE(6,41)
                WRITE(6,48)
                WRITE(6,41)
                WRITE(6,86)
                WRITE(6,83)JCOMP
                WRITE(6,86)
                WRITE(6,41)
                WRITE(6,86)
                WRITE(6,84)
                WRITE(6,86)
                WRITE(6,41)
                WRITE(6,86)
                WRITE(6,73)
                WRITE(6,84)
                WRITE(6,41)
                WRITE(6,86)
             40 FORMAT('1',////////)
             41 FORMAT(1PX,98(1H0))
             42 FORMAT(1PX,'0',49X,'ABSOLUTE VALUES',41X,'0')
             43 FORMAT(1PX,'0',7X,'TIME',13X,'D(MV)',13X,'RMOLE',13X,'PA(MM HG)',7
            2X,'CONC(G-MOLE/CC)',1X,'0')
             44 FORMAT(1PX,'0',2X,6(D12.5,8X),D12.5,2X,'0')
             45 FORMAT(1PX,'0',49X,'RUN CODE=',I3,49X,'0')
             46 FORMAT(1PX,'0',49X,'DEVIATION VALUES',49X,'0')
             47 FORMAT(1PX,'0',7X,'TIME',14X,'RMOLE0',13X,'PA(MM HG)',8X,'CONC(G-M
            2OLE/CC)',7X,'CONCDIFF',4X,'0')
                DO 10 J=1,M
                RMOLER(J)=DABS(RMOLE(J)-RMOLE(1))
                PAD(J)= DABS(PA(J)-PA(1))
                CONCD(J)= PABS (CONC(J)-CONC(1))
                P(J)= CONCD(J)*TIME(J)
                V(J)=P(J)*T(MR(J)
                WRITE(6,44)TIME(J),RMOLE0(J),PAD(J),CONCD(J),P(J)
             10 CONTINUE
                WRITE(6,86)
                WRITE(6,41)
                UM= DCSIGU (CONCD,TIME,M,M,IER)
                UI= DCSIGU(P,TIME,M,M,IER)
                UE= DCSIGU(V,TIME,M,M,IER)
                UVI= UI/UO
                UVD=UD/UO
                UVC=UVE-UVI=UV1
                CONCIN= RMOLIN*PRESS/R/TEMP
                CONCPP=RMOLPP*PRESS/R/TEMP
                TAUP= VPLUG/PLOW
                VETAR= AREA*L
                TAUD= VETAR/PLOW
                RSTEP= DABS(CONCIN-CONCPP)
                DM = RSTEP*U
```

```
0176                  DC(INV=1)0.0)) 0 XMPLOT(1)/YMOLIN
0177                  TC(YW=1)0.0)0UA/DR
0178                  WR(R)= UR/YM
0179                  SS = PLAN/SORPA
0180            101   FORMAT(1HX,'0',8X,8(1X)0.0,8X);D10.0,8X,'0')
0181                  RP(R)=RM(R)/PLOT(1.,100-MM(R))
0182                  PM(R)=RRRRRR PM(R)00.000
0183                  RR(R)=(RM(R)-1.000)/TAUB
0184                  WR(R)= (UV)-TAUM*(0.,RR0-RR(R))-W/0.0001/TAUB
0185                  CC(R)=RMAL(I)
0186                  WR(TP(0,10)
0187                  WR(TP(0,07)
0188                  WR(TP(0,00) SCALPP
0189                  WR(TP(0,02)
0190                  WR(TP(0,01) TIMP
0191                  WR(TP(0,07)
0192                  WR(TP(0,00)PLOT
0193                  WR(TP(0,07)
0194                  WR(TP(0,01)M
0195                  WR(TP(0,07)
0196                  WR(TP(0,00)V
0197                  WR(TP(0,07)
0198                  WR(TP(0,00) UR
0199                  WR(TP(0,07)
0200                  WR(TP(0,01) UI
0201                  WR(TP(0,07)
0202                  WR(TP(0,00) UVI
0203                  WR(TP(0,07)
0204                  WR(TP(0,03)UB
0205                  WR(TP(0,07)
0206                  WR(TP(0,04)UVB
0207                  WR(TP(0,07)
0208                  WR(TP(0,05)UVC
0209                  WR(TP(0,07)
0210                  WR(TP(0,01) RETEP
0211                  WR(TP(0,07)
0212                  WR(TP(0,06) TM
0213                  WR(TP(0,02)
0214                  WR(TP(0,06) TCONV
0215                  WR(TP(0,07)
0216                  WR(TP(0,06) QCONV
0217                  WR(TP(0,07)
0218                  WR(TP(0,07) CUMC(I)
0219                  WR(TP(0,07)
0220                  WR(TP(0,07)
0221            00    FORMAT(1H1,'0',8X,'PHOCALEP=',D12.0,8X,'0')
0222            01    FORMAT(1H1,'0',8X,'HTINEP=',D12.0,8X,'0')
0223            00    FORMAT(1H1,'0',8X,'AMPLOD',1X,'=',D12.0,8X,'0')
0224            02    FORMAT(1H1,'0',8X,'MM',8X,'=',D12.0,8X,'0')
0225            01    FORMAT(1H1,'0',8X,'MM',8X,'=',I2,8X,'0')
0226            03    FORMAT(1H1,'0',8X,'RMS',8X,'=',D12.0,8X,'0')
0227            04    FORMAT(1H1,'0',8X,'RMSV',8X,'=',D12.0,8X,'0')
0228            05    FORMAT(1H1,'0',8X,'RMSVE',8X,'=',D12.0,8X,'0')
0229            06    FORMAT(1H1,'0',8X,'0')
```

```
PRINTMAN IV 01   RELEASE 2.0              MAIN              DATE = 78216        10/30/19                PAGE 0001

 0100            97    FORMAT(6(X,'0',8RR,'0'))
 0110            98    FORMAT(1(X,'0',1(1X,'0'))
 0120            99    FORMAT(1HF,'0',80X,'PARAMETER GROUP NUMBERS AS FUNCTION OF OUTLET
                      1WALFRACTION',21X,'0')
 0130            01    FORMAT(6(1X,'0',8X,8HUG,3X,'0',D12.5,8X,'0'))
 0140            01    FORMAT(6(1X,'0',8X,8HUI,3X,'0',D12.5,8X,'0'))
 0150            98    FORMAT(6(1X,'0',8X,8HUVI,3X,'0',D12.5,8X,'0'))
 0160            01    FORMAT(6(1X,'0',8X,8HRSTEP,3X,D12.5,8X,'0'))
 0170            04    FORMAT(6(1X,'0',8X,8HRR,3X,'0',D12.5,8X,'0'))
 0180            05    FORMAT(6(1X,'0',8X,8HTCONV,3X,D12.5,8X,'0'))
 0190            06    FORMAT(6(1X,'0',8X,8HDCONV,3X,D12.5,8X,'0'))
 0200            07    FORMAT(6(1X,'0',8X,8HCEQUT,3X,D12.5,8X,'0'))
 0210            08    FORMAT(1HF,'0',8X,'HNOUT',13X,'NP',13X,'NR',13X,'NN',13X,'NO',13X,
                      1'RP',2X,'0')
 0220                  WRITE(6,100)IPR
 0230            100   CONTINUE
 0240                  WRITE(6,400)
 0250                  WRITE(6,310)
 0260                  WRITE(6,98)
 0270                  WRITE(6,99)
 0280                  WRITE(6,310)
 0290                  WRITE(6,99)
 0300                  WRITE(6,98)
 0310                  WRITE(6,310)
 0320                  WRITE(6,98)
 0330                  DO 900 KK=1,IR
 0340                  WRITE(6,1001) CC(KK),RP(KK),DR(KK),RN(KK),RG(KK),RPIRK)
 0350            900   CONTINUE
 0360                  WRITE(6,98)
 0370                  WRITE(6,310)
 0380            310   FORMAT(1HF,103(1H0))
 0390            100   FORMAT(//////////////,48X,'INTEGRATION ERROR CHECK ITERN',I3)
 0400            1000  CONTINUE
 0401                  STOP
 0402                  END

 *OPTIONS IN EFFECT*   NOTRAN,ID,FSCD(C,SOURCE,NOLIST,NODECK,LOAD,NOMAP,NOTEST
 *OPTIONS IN EFFECT*   NAME = MAIN    , LINECNT =      56
 *STATISTICS*     SOURCE STATEMENTS =      402,PROGRAM SIZE =    20480
 *STATISTICS*  NO DIAGNOSTICS GENERATED
```

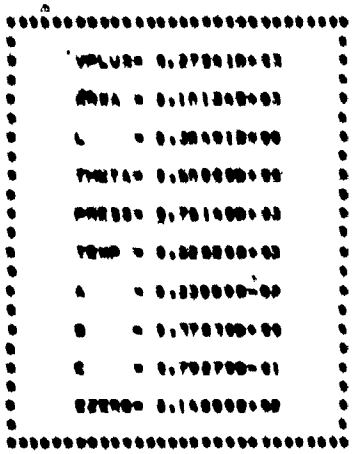

RUN CODE=170

ABSOLUTE VALUES

TIME	R(INV)	RADIUS	PA(MM HG)	CONC(G-MOLS/CC)
0.0	0.000000+01	0.000000+00	0.176670+03	0.000000-00
0.100000+02	0.000000+01	0.000000+00	0.176670+03	0.000000-00
0.200000+02	0.000000+01	0.000000+00	0.176670+03	0.000000-00
0.300000+02	0.000000+01	0.000000+00	0.176670+03	0.000000-00
0.400000+02	0.000000+01	0.000000+00	0.176670+03	0.000000-00
0.500000+02	0.000000+01	0.000000+00	0.176670+03	0.000000-00
0.600000+02	0.000000+01	0.000000+00	0.176670+03	0.000000-00
0.700000+02	0.000000+01	0.000000+00	0.176670+03	0.000000-00
0.800000+02	0.000000+01	0.000000+00	0.176670+03	0.000000-00
0.900000+02	0.000000+01	0.000000+00	0.176670+03	0.000000-00
0.100000+03	0.000000+01	0.000000+00	0.176670+03	0.000000-00
0.110000+03	0.000000+01	0.000000+00	0.176670+03	0.000000-00
0.120000+03	0.000000+01	0.000000+00	0.176670+03	0.000000-00
0.130000+03	0.000000+01	0.000000+00	0.176670+03	0.000000-00
0.140000+03	0.000000+01	0.000000+00	0.176670+03	0.000000-00
0.150000+03	0.000000+01	0.000000+00	0.176670+03	0.000000-00
0.160000+03	0.000000+01	0.000000+00	0.176670+03	0.000000-00
0.170000+03	0.000000+01	0.000000+00	0.176670+03	0.000000-00
0.180000+03	0.000000+01	0.000000+00	0.176670+03	0.000000-00
0.190000+03	0.000000+01	0.000000+00	0.176670+03	0.000000-00
0.200000+03	0.000000+01	0.000000+00	0.176670+03	0.000000-00

RUN COMPLETE

DEVIATION VALUES

TIME	ANGLE	RATE RAD	CONCEN-MOLE/CC	CONCENTRATION
0.0	0.0	0.0	0.0	0.0
0.100000+00	0.000000E-00	0.200000E+01	0.000000E-00	0.000000E-00
0.200000+00	0.000000E-00	0.200000E+01	0.000000E-00	0.000000E-00
0.300000+00	0.000000E-00	0.200000E+01	0.000000E-00	0.000000E-00
0.400000+00	0.000000E-00	0.200000E+01	0.000000E-00	0.000000E-00
0.500000+00	0.000000E-00	0.200000E+01	0.000000E-00	0.000000E-00
0.600000+00	0.000000E-00	0.200000E+01	0.000000E-00	0.000000E-00
0.700000+00	0.000000E-00	0.200000E+01	0.000000E-00	0.000000E-00
0.800000+00	0.000000E-00	0.200000E+01	0.000000E-00	0.000000E-00
0.900000+00	0.000000E-00	0.200000E+01	0.000000E-00	0.000000E-00
0.100000+01	0.000000E-00	0.200000E+01	0.000000E-00	0.000000E-00
0.110000+01	0.000000E-00	0.200000E+01	0.000000E-00	0.000000E-00
0.120000+01	0.000000E-00	0.200000E+01	0.000000E-00	0.000000E-00
0.130000+01	0.000000E-00	0.200000E+01	0.000000E-00	0.000000E-00
0.140000+01	0.000000E-00	0.200000E+01	0.000000E-00	0.000000E-00
0.150000+01	0.000000E-00	0.200000E+01	0.000000E-00	0.000000E-00
0.160000+01	0.000000E-00	0.200000E+01	0.000000E-00	0.000000E-00
0.170000+01	0.000000E-00	0.200000E+01	0.000000E-00	0.000000E-00
0.180000+01	0.000000E-00	0.200000E+01	0.000000E-00	0.000000E-00
0.190000+01	0.000000E-00	0.200000E+01	0.000000E-00	0.000000E-00
0.200000+01	0.000000E-00	0.200000E+01	0.000000E-00	0.000000E-00
0.210000+01	0.000000E-00	0.200000E+01	0.000000E-00	0.000000E-00
0.220000+01	0.000000E-00	0.200000E+01	0.000000E-00	0.000000E-00
0.230000+01	0.000000E-00	0.200000E+01	0.000000E-00	0.000000E-00
0.240000+01	0.000000E-00	0.200000E+01	0.000000E-00	0.000000E-00
0.250000+01	0.0	0.0	0.0	0.0

4423961

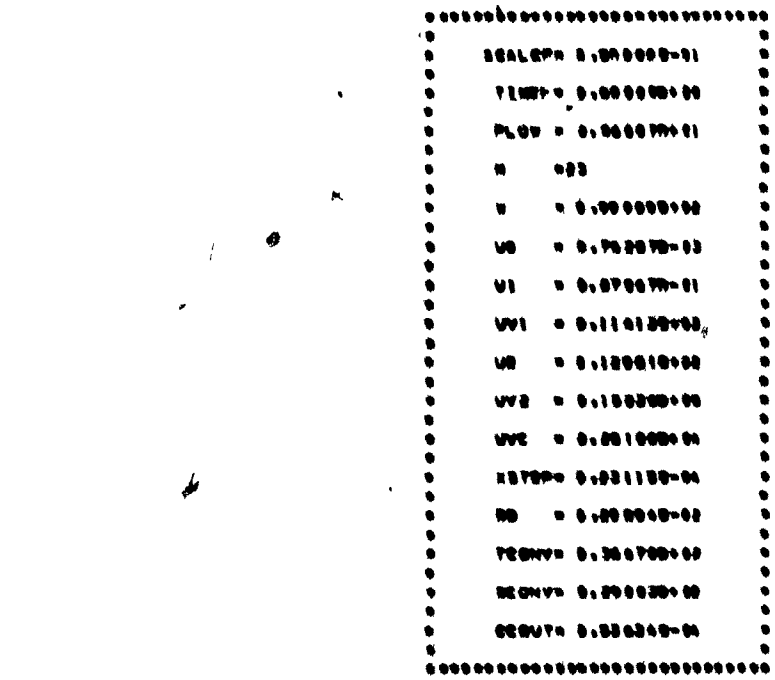

INTEGRATION ERROR CHECK (IER) 0

APPENDIX A

FIGURE A-2 Programme listings for the estimation of the parameters from the parameter groups and a sample output.

```
FORTRAN IV G1  RELEASE 2.0            MAIN             DATE = 72244      11/04/09          PAGE 0001

                C     SOLUTION OF TWO NON-LINEAR EQUATIONS USING TWO
                C     REGULA FALSI TECHNIQUES TO OBTAIN THE TWO PARAMETERS WHICH ARE
                C     RAM = REACTION RATE CONSTANT (1/SEC)
                C     D = INTRA PARTICLE DIFFUSIVITY (SQ.CM/SEC)
                C     PHIP = DIMENSION LESS ROOT FOR PRODUCT(CHARACTERISTIC)
                C     PHIDRL= DIMENSION LESS ROOT FOR REACTANT(CHARACTERISTIC)
0001                  IMPLICIT REAL*8(A-H,L,O-Z),INTEGER*4(I-K,N)
0002                  DIMENSION RP(2,20),RR(2,20),RM(2,20),RO(2,20),RP(2,20),CONC(20),RI
                     1(20),RAR(20),PHIP(20),PHIDRL(20)
0003                  EXTERNAL F
0004                  COMMON L1, L2, RATIO
0005                  L2=0.2E-01
0006                  ARGAM(0).DA
0007                  L1=0.1E2
0008                  READ(5,1) IN
0009                  READ(5,1) K
0010             1    FORMAT(I2)
0011                  DO 100 KK=1,IN
0012                  READ(5,2) TEMP
0013                  DO 10 I=1,K
0014            10    READ(5,3) CONC(I)
0015            3     FORMAT(D10.3)
0016                  DO 20 I=1,2
0017                  READ(5,4) PL,RR
0018                  READ(5,4) AR,BR
0019                  READ(5,4) AM, BM
0020                  READ(5,4) AO, BO
0021                  READ(5,4) AP, BP
0022             4    FORMAT(2D10.10)
0023                  DO 30 J=1,K
0024                  RR(I,J)=AR+BR*CONC(J)
0025                  RP(I,J)=RR(I,J)*PL*EXP(I,ORD=RR(I,J))
0026                  RM(I,J)=0.5D0*RR(I,J)*PL*EXP*PL*EXP/AREA/AREA
0027                  RO(I,J)=AM+BM*CONC(J)
0028                  RP(I,J)=AP+BP*CONC(J)
0029            30    CONTINUE
0030            20    CONTINUE
                C     SOLUTION OF THE FIRST EQUATION
0031                  DO 40 J=1,K
0032                  EPS=10D-07
0033                  IETA=0
0034                  ITMAX=1000
0035                  A=1.D00
0036                  B=50.D00
0037                  RATIO=RP(1,J)/RP(2,J)
0038                  WRITE(6,71)
0039                  WRITE(6,69)
0040                  WRITE(6,70)
0041                  WRITE(6,72) TEMP
0042                  WRITE(6,70)
0043                  WRITE (6,69)
0044                  WRITE(6,70)
0045                  M=1
0046                  JJ=2
```

```
FORTRAN IV G1  RELEASE 2.0            MAIN            DATE = 78266        11/09/58                PAGE 0004

0047                  WRITE(6,66)M,JL
0048                  WRITE(6,70)
0049                  WRITE(6,69)
0050                  WRITE(6,70)
0051                  WRITE(6,64) (ANG(J)
0052                  WRITE(6,70)
0053                  WRITE(6,73) RATIO
0054                  WRITE(6,70)
0055                  WRITE(6,60) RP(1,J),RP(2,J)
0056                  WRITE(6,70)
0057                  WRITE(6,61) RR(1,J),RR(2,J)
0058                  WRITE(6,70)
0059                  WRITE(6,62) RH(1,J),RH(2,J)
0060                  WRITE(6,70)
0061                  WRITE(6,63) RQ(1,J),RQ(2,J)
0062                  WRITE(6,70)
0063                  WRITE(6,64) RP(1,J),RP(2,J)
0064                  WRITE(6,70)
0065                  CALL ZERONT(P,EPS,1010,4,0,ITMAX,IER)
0066                  WRITE(6,67) R
0067                  WRITE(6,70)
0068                  PSUP(10)
0069                  WRITE(6,74) PS
0070                  WRITE(6,70)
0071                  IF(IER.EQ.128) GO TO 11
0072                  IF(IER.EQ.130) GO TO 12
0073                  GO TO 14
0074            11    WRITE(6,13)
0075                  GO TO 50
0076            13    FORMAT('0',20X,'ALGORITHM FAILED TO CONVERGE IN ITMAX ITERATIONS')
0077            12    WRITE(6,15)
0078                  GO TO 50
0079            15    FORMAT('0',20X,'NO ROOT(META) TO BE FOUND FOR THE SPECIFIED RANGE')
0080            14    ARG1=A1*B
0081                  ARG2=A2*B
0082                  GAM1= RP(1,J)/AREA/GTAMM(ARG1)
0083                  GAM2= RP(2,J)/AREA/GTAMM(ARG2)
                      SOLUTION OF THE SECOND EQUATION
0084                  GG1= 0.5000*(RQ(1,J)  + R * GAM1*(1.000/RR(1,J)-RR(1,J)))
0085                  GG2=0.5000*(RQ(2,J)+R*GAM2*(1.000/RR(2,J)-RR(2,J)))
0086                  GG= GG1-GG2
0087                  GM1=RH(1,J)/R*GAM1
0088                  GM2=RH(2,J)/R*GAM2
0089                  AA=GM1-GM2
0090                  BB=RP(1,J)-RP(2,J)
0091                  DET=BB*BB-4.0000*AA*CC
0092                  IF(DET.LT.0.000) GO TO 120
0093                  RAR1=(BB+DSQRT(DET))/(2.0000*AA)
0094                  RAR2=(BB-DSQRT(DET))/(2.0000*AA)
0095                  RQ(1)=RP(1,J)-GM1*RAR1*RAR1/RAR1
0096                  RQ(2)=RP(1,J)-GM2*RAR2*RAR2/RAR2
0097                  RQ2DL2=R*GAM2/RAR2
0098                  RQ2DL1=R*GAM1/RAR1
0099                  GA=GGG

4853-78
```

```
FORTRAN IV G1  RELEASE 2.0            MAIN            DATE = 78168        11/58/48        PAGE 0001

0100                  DIP1=PAR1/RA
0101                  DIP2=PAR2/RA
0102                  WRITE(6,65) ANG1, ANG2
0103                  WRITE(6,70)
0104                  WRITE(6,90) GAM1,GAM2
0105                  WRITE(6,70)
0106                  WRITE(6,97) G01, G02
0107                  WRITE(6,70)
0108                  WRITE(6,98) GN1, GN2
0109                  WRITE(6,70)
0110                  WRITE(6,49)
0111                  WRITE(6,70)
0112                  WRITE(6,67)
0113                  WRITE(6,70)
0114                  WRITE(6,49)
0115                  WRITE(6,70)
0116                  WRITE(6,60) PAR1, PAR2
0117                  WRITE(6,70)
0118                  WRITE(6,61) PSIP1, PSIP2
0119                  WRITE(6,70)
0120                  WRITE(6,62) PSIDL1, PSIDL2
0121                  WRITE(6,70)
0122                  WRITE(6,63) DIP1,DIP2
0123                  WRITE(6,70)
0124                  WRITE(6,49)
0125                  GO TO 40
0126            120   WRITE(6,110)
0127            40    CONTINUE
0128           110    FORMAT('0',10X,'NO SOLUTION FOR QUADRATIC EQUATION')
0129            71    FORMAT('1',////////)
0130            49    FORMAT(41X,63('='))
0131            70    FORMAT(41X,'0',61X,'0')
0132            72    FORMAT(41X,'0',20X,'TEMPERATURE=',D10.5,10X,'0')
0133            66    FORMAT(41X,'0',9X,11,21X,11,11X,'0')
0134            59    FORMAT(41X,'0',5X,2HMF,15X,D12.5,10X,D12.5,5X,'0')
0135            61    FORMAT(41X,'0',5X,2HMA,15X,D12.5,10X,D12.5,5X,'0')
0136            62    FORMAT(41X,'0',5X,2HMN,15X,D12.5,10X,D12.5,5X,'0')
0137            63    FORMAT(41X,'0',5X,2HMO,15X,D12.5,10X,D12.5,5X,'0')
0138            64    FORMAT(41X,'0',5X,2HMP,15X,D12.5,10X,D12.5,5X,'0')
0139            65    FORMAT(41X,'0',5X,3HANG,14X,D12.5,10X,D12.5,5X,'0')
0140            96    FORMAT(41X,'0',5X,3HGAM,14X,D12.5,10X,D12.5,5X,'0')
0141            97    FORMAT(41X,'0',5X,3HG0,15X,D12.5,10X,D12.5,5X,'0')
0142            98    FORMAT(41X,'0',5X,2HGN,15X,D12.5,10X,D12.5,5X,'0')
0143            67    FORMAT(41X,'0',20X,'ESTIMATED PARAMETERS',21X,'0')
0144            68    FORMAT(41X,'0',5X,'K',16X,D12.5,10X,D12.5,5X,'0')
0145            61    FORMAT(41X,'0',5X,'PSIP',13X,D12.5,10X,D12.5,5X,'0')
0146            62    FORMAT(41X,'0',5X,'PSIDEL',11X,D12.5,10X,D12.5,5X,'0')
0147            63    FORMAT(41X,'0',5X,'DIP',14X,D12.5,10X,D12.5,5X,'0')
0148            64    FORMAT(41X,'0',5X,'KNOUT',12X,D12.5,27X,'0')
0149            68    FORMAT(41X,'0',5X,'B',16X,D12.5,27X,'0')
0150            74    FORMAT(41X,'0',5X,'F',16X,D12.5,27X,'0')
0151            73    FORMAT(41X,'0',5X,'RATIO',12X,D12.5,27X,'0')
0152           100    CONTINUE
0153                  STOP
```

```
FORTRAN IV G1  RELEASE 2.0              P                    DATE = 78204     11/58/40          PAGE 0001

0001                  FUNCTION P(BETA)
0002                  IMPLICIT REAL*8(A-H,L,N-S),INTEGER(I-K,M)
0003                  COMMON L1, LR, RATIO
0004                  P=BETAH(L1*BETA)-RATIO*BETAH(LR*BETA)
0005                  RETURN
0006                  END

 *OPTIONS IN EFFECT*   NOTERM,ID,EBCDIC,SOURCE,NOLIST,NODECK,LOAD,NOMAP,NOTEST
 *OPTIONS IN EFFECT*   NAME = P       , LINECNT =      56
 *STATISTICS*  SOURCE STATEMENTS =          6,PROGRAM SIZE =      400
 *STATISTICS*  NO DIAGNOSTICS GENERATED

 *STATISTICS*  NO DIAGNOSTICS THIS STEP
```

TEMPERATURE=.233000+01

KMAT	0.400000-01	
RATIO	0.000400+00	
MP	0.300000+00	0.365470+00
MM	0.373000-01	0.418970-01
MM	0.130200-03	0.149000-03
MQ	-0.611000+00	-0.218830+01
MP	-0.870200+01	-0.107100+01
B	0.110700+02	
F	0.000230-07	
ARG	0.140200+01	0.420400+01
GAM	0.300000-02	0.300000-07
GQ	0.200230+00	0.367100+00
GM	0.420410-07	0.000010-07

ESTIMATED PARAMETERS

K	0.727300-01	0.471710+00
PSIP	-0.001000+01	-0.277170+02
PSIDEL	0.000000+00	0.000030-10
DIP	0.000000-03	0.304300+07

4853416